Amino Acids (2005) 29: 355–376
DOI 10.1007/s00726-005-0237-2

Amino Acids
Printed in Austria

Small animal positron emission tomography in food sciences

Review Article

R. Bergmann and **J. Pietzsch**

Positron Emission Tomography Center, Institute of Bioinorganic and Radiopharmaceutical Chemistry, Research Center Rossendorf, Dresden, Germany

Received June 1, 2005
Accepted July 13, 2005
Published online September 2, 2005;

Summary. Positron emission tomography (PET) is a 3-dimensional imaging technique that has undergone tremendous developments during the last decade. Non-invasive tracing of molecular pathways *in vivo* is the key capability of PET. It has become an important tool in the diagnosis of human diseases as well as in biomedical and pharmaceutical research. In contrast to other imaging modalities, radiotracer concentrations can be determined quantitatively. By application of appropriate tracer kinetic models, the rate constants of numerous different biological processes can be determined. Rapid progress in PET radiochemistry has significantly increased the number of biologically important molecules labelled with PET nuclides to target a broader range of physiologic, metabolic, and molecular pathways. Progress in PET physics and technology strongly contributed to better scanners and image processing. In this context, dedicated high resolution scanners for dynamic PET studies in small laboratory animals are now available. These developments represent the driving force for the expansion of PET methodology into new areas of life sciences including food sciences. Small animal PET has a high potential to depict physiologic processes like absorption, distribution, metabolism, elimination and interactions of biologically significant substances, including nutrients, 'nutriceuticals', functional food ingredients, and foodborne toxicants. Based on present data, potential applications of small animal PET in food sciences are discussed.

Keywords: Positron emission tomography – Food sciences – Small animal PET scanners – PET tracer

1 Introduction

For more than 20 years positron emission tomography (PET) has been a powerful imaging technique in the diagnosis of human diseases as well as in biomedical research. PET methodology is based on the administration of a tracer compound labelled with positron-emitting nuclides such as carbon-11 ($t_{1/2} = 20.39$ min), nitrogen-13 ($t_{1/2} = 9.97$ min), oxygen-15 ($t_{1/2} = 2.04$ min), and fluorine-18 ($t_{1/2} = 109.77$ min). In tissue, annihilation of an emitted positron with an electron results in the simultaneous emission of two 511 keV photons under a relative angle of 180°. These two annihilation photons are recorded by coincidence detection (i.e. simultaneous detection by two opposing detectors). These two detectors define the line of response along which the original annihilation took place. As the total path length of both annihilation photons together is also known, accurate correction of attenuation of the radiation during its passage through tissue is possible. In this way, after administration of a radiolabelled substance of interest, the distribution of the radioactivity in the different organs and tissues is measured. Using dynamic data acquisition protocols time-activity curves of radioactivity uptake in several body compartments can be obtained. Measurements of tracer concentrations in these compartments can be translated into quantitative values of the biochemical activity of cells, tissues, and organs with the help of suitable tracer kinetic models if plasma concentration of the tracer and its metabolites are measured simultaneously by taking blood samples.

PET is used primarily in oncology, neurology, cardiology, and rheumatology. Thus, PET is focused on the detection and staging of primary tumours and metastases, the assessment of potential benefits of coronary artery bypass surgery, the evaluation of a variety of neurodegenerative disorders, and the detection of local and systemic inflammatory processes. Traditional medical diagnostic imaging modalities, such as X-ray computed tomography (CT) and magnetic resonance imaging (MRI), produce

images of the body's anatomy or morphology. In contrast, PET visualizes the body's biochemistry that, in the diseased state, may be altered prior to any change in gross anatomy, thus allowing early diagnosis of processes of pathophysiologic relevance (Cherry, 2001; Johannsen, 2005). For example, molecular changes in cancer occur up to 6 years before a mass becomes visible. Detection of molecular signatures permits diagnosis at a much earlier stage of the disease, leading to an earlier treatment and an improved prognosis.

In this context, the PET technique has been optimized for human applications. However, far reaching progress in PET technology has also led to the design and development of dedicated small animal PET systems that now are increasingly prevalent in biomedical and pharmaceutical research. These small animal PET systems enable researchers to perform dynamic PET studies with high spatial and temporal resolution in small laboratory animals such as mice and rats (Chatziioannou, 2002a, b; Cherry and Gambhir, 2001; Roselt et al., 2004; Rowland et al., 2002; Weber and Bauer, 2004). Notably, dynamic PET studies can be performed in classical design by single measurements as well as of longitudinal design that are characterised by repeated measurements in a single animal (Moore et al., 2000).

Beside commercial availability of small animal PET systems, progress in PET radiochemistry has further promoted this field (Wuest, 2005). The most prominent PET tracer is the ^{18}F-labelled glucose analogue 2-deoxy-2-[^{18}F]fluoro-D-glucose (FDG). FDG is characterized by its high accumulation in brain, heart or tumour tissue based on the higher glucose transport and metabolism rate in these tissues. The quantification of FDG uptake is based on Sokoloff's method, which was developed by using [^{14}C]deoxyglucose (Sokoloff, 1976; Sokoloff et al., 1977). The plethora of new PET tracers can be subdivided into three categories: *a*) those that trace non-saturable physiological and biochemical processes, e.g., accumulation of [^{18}F]fluoride in bone, *b*) intermediately saturable systems, e.g., accumulation of FDG as a measure of glucose transporter and hexokinase activity, and *c*) easily saturable, low-density systems, e.g., ^{18}F-labelled vasoactive intestinal peptide (VIP), a radioligand to measure VIP receptor density in tumours (Jagoda et al., 2002). It could be demonstrated that many PET radiopharmaceuticals can be obtained at high specific radioactivity that application of a human dose into a mouse or rat has no effect on the pharmacokinetics for non-saturable or high capacity sites. For receptor binding radioligands, however, the present effective specific activity of radiopharmaceuticals, which depends not only on the specific activity of the radiopharmaceutical itself but also on the endogenous receptor ligand concentration, could lead to partial saturation of the target site. In this case, both, an increase of the specific activity of the PET tracer and an increase of the sensitivity of the small animal PET scanners in relation to the human scanners will be necessary to study the receptor interactions by using small animal PET (Jagoda et al., 2004).

The extremely broad spectrum of potential PET tracers and the nearly unlimited range of physiological, biochemical, and pharmacokinetic parameters that can be measured stems from the fact that, in principle, virtually all biological molecules can be labelled with positron emitters carbon-11, nitrogen-13, and oxygen-15 that represent the elements of life. In addition, fluorine-18 is often used as a substitute of hydrogen, which itself does not have a positron emitting isotope. A further assumption behind the labelling with fluorine-18 is that in various molecules fluorine atoms can be substituted for hydroxy groups with acceptable alteration of the behaviour of the molecule in the living organism.

All these facts provide the technical and scientific basis for expansion of small animal PET into various fields of food sciences.

2 Recent developments in small animal PET methodology

Small laboratory animals such as mice or rats, but also hamsters, rabbits, minipigs, and primates, are widely used in biomedical research because of their genetic resemblance to humans, and to mimic human subjects for both healthy and diseased states. Very recently, various small animal models of disease including genetically-modified animals have been developed (Bocan, 1998; German and Eisch, 2004; Lyons, 2005). Studies of these animals with small animal PET scanners are likely to provide new insights in molecular processes *in vivo* with regard, for instance, to food evaluation or nutritional studies (Boisgard et al., 2003; Herschman, 2003; Knoess et al., 2003; Roselt et al., 2004; Tawakol et al., 2005; van Kouwen et al., 2005; Weber and Bauer, 2004; Yang et al., 2004).

Several PET scanners dedicated to animal work have been developed so far with different technical characteristics. These PET scanners comprise both a number of research prototypes and systems of second generation like SHR-7700 (Hamamatsu, Japan), Sherbrooke Animal PET (Sherbrooke, Canada), RATPET (MRC Hammersmith, UK), TierPET (Jülich, Germany), YAP-PET (Ferrara,

Italy), MAD-PET (Munich, Germany), ANI-PET (Montreal, Canada), and ClearPET (Straubenhardt, Germany) (Auffray et al., 2004; Heinrichs et al., 2004; Knoess et al., 2003; Lecomte, 1992, 2004; McElroy et al., 2005; Schafers, 2003; Seidel et al., 2003; Surti et al., 2003; Tai et al., 2003, 2005; Vaska et al., 2004; Weber et al., 1997; Weber and Bauer, 2004; Ziemons et al., 2005). Nowadays the broad application of animal PET studies was stimulated by the availability of various commercially available scanners, including the microPET system series (CTI Concorde Microsystems, USA) and the quadHIDAC system (Oxford Positron Systems Ltd, UK) (Chatziioannou et al., 2001; Chatziioannou, 2002b; Yang et al., 2004). Among these systems, the microPET Focus system (CTI Concorde Microsystems, USA) represents the latest generation of small animal PET scanners. This system incorporates several changes in design that significantly improve its performance when compared with previous models (Tai et al., 2005). As an example, the microPET Focus consists of 24,129 lutetium oxyorthosilicate (LSO) crystals each measuring $1.51 \times 1.51 \times 10.00\,\mathrm{mm}^3$, which are arranged in 48 contiguous rings, with 504 crystals per ring. The scanner has an axial field of view (FOV) of 7.6 cm and a transaxial FOV of 19.0 cm. The scintillation light is transmitted to position-sensitive photomultiplier tubes via optical fiber bundles. The energy resolution averages 18.5% for the entire system. Reconstructed image resolution is 1.3-mm full width at half maximum (FWHM) at the center of the field of view (CFOV). It remains under 2 mm FWHM within the central 5-cm-diameter FOV in all 3 dimensions. The absolute sensitivity of the system is 3.4% at the CFOV for an energy window of 250–750 keV and a time window of 10 ns. The noise equivalent counting-rate performance reaches 645 kcps for a mouse-size phantom using 250 to 750 keV and 6-ns settings. In summary, this system represents the state-of-the-art scintillator-based animal PET scanner currently available and is expected to further advance the potential of small animal PET.

A complete PET procedure includes data acquisition, conversion of the list mode data into time intervals (frames), generation of sinograms, reconstruction of image, and the qualitative and quantitative analysis of temporal and spatial radioactivity distribution. Many factors influence the quality and accuracy of the resulting images. This begins with the experimental setup, like size of the animal, absolute amount of administrated radioactivity, radioactivity concentration in tissues or organs of interest, the contrast between the radioactivity in target tissues and background radioactivity of the vicinity. Physical effects like background radioactivity, attenuation, and scattering are important. The geometry of the scanner detectors influences the geometric resolution. The image reconstruction algorithms, like single slice rebinning (SSRB) methods, Fourier rebinning (FORE) methods, two- (2-D) or three-dimensional (3-D) ordered-subsets expectation-maximization (OSEM) algorithms, have their advantages and disadvantages for each individual experimental situation (Defrise et al., 1997; Farquhar et al., 1998; Liu et al., 2001; Weber et al., 1997; Yao et al., 2000).

The qualitative evaluation of biological situations and the quantitative description of the accompanied cellular and molecular biochemical processes in health and diseases are, at least, the main aims of PET investigations. The capabilities of quantitative imaging by PET are depending on the scanner used, on the particular application, on factors influencing the data acquisition, and on the further data management and calculation algorithms as discussed in detail elsewhere in this issue (van den Hoff, 2005). The main factors influencing the quantitative accuracy in the imaging process are presented in Table 1. There are three grades of quantitative evaluation of PET studies: *a*) calculation of the radioactivity distribution in the tissues of interest, expressed as the radioactivity concentration, given as percentage of injected dose per cubic centimetre (%ID/cm^3) or as percentage of injected dose (%ID) alone, *b*) estimation of regions of interest based non-compartmental or compartmental derived kinetic parameters from dynamic studies, and/or *c*) estimation of pixel based non-compartmental or compartmental derived kinetic parameters from dynamic studies and presentation as parameter images. In small animal PET studies, the

Table 1. Factors influencing the quantitative imaging and parameter estimation by PET

Quantitative imaging
Dynamic imaging
Radioactive decay correction
Dead-time correction
Attenuation and scatter correction
Activity calibration (in Bq/mL or nCi/mL)
Parameter estimation
Activity calibration (in Bq/mL or nCi/mL)
Recovery correction
Partial-volume correction
Arterial input curve
Activity calibration
Delay correction
Dispersion correction
Metabolite analysis in the arterial plasma samples

data to be analysed typically were derived from the 3-dimensional images. To capture the information from these PET images one needs to mark 3-dimensional regions of interest (ROIs) or volumes of interest (VOIs) and to receive the radioactivity concentration and the volume of each ROI or VOI. To measure the activity distribution also in complex geometric structures, e.g., quantification of PET tracer elimination into the intestine, it is necessary to use specialized programs, which with minimal user interaction allow the creation of multiple ROIs and the segmentation of the activity including background subtraction (Poetzsch et al., 2003). An automated method for placement of 3-dimensional rat brain atlas-derived VOIs onto PET studies has been designed and evaluated. VOIs representing major structures of the rat brain were defined on a set of digitized cryosectioned images of the rat brain. For VOI placement, each PET study was registered with a synthetic PET target constructed from the VOI template. Registration was accomplished with an automated algorithm that maximized the mutual information content of the image volumes. The accuracy and precision of this method for VOI placement was determined using datasets from PET studies of the striatal dopamine and hippocampal serotonin systems. Each evaluated PET study could be registered to at least one synthetic PET target without obvious failure. Registration was critically dependent upon the initial position of the PET study relative to the synthetic PET target, but independent on the amount of synthetic PET target smoothing. An evaluation algorithm showed that resultant radioactivity concentration measurements of selected brain structures contained errors that equal 2% due to misalignment to the corresponding VOI. Further, radioligand binding values calculated from these measurements were found to be more precise than those calculated from measurements obtained with manually drawn regions of interest (ROIs). Overall, evaluation results demonstrated that this atlas-derived VOI method could be used to obtain unbiased measurements of radioactivity concentration from PET studies. Its automated features and applicability to different radioligands and brain regions will facilitate quantitative rat brain PET assessment procedures (Rubins et al., 2003).

Dependent on the resulting ROI volume it is necessary to include calculations of the recovery correction when the ROI volume is roughly lower than three times of the volume resolution calculated from the efficient FWHM at the present position and used reconstruction algorithm. Up to now the problem of partial volume correction, which means the correction for overspill between the surrounding and the target structure, for small ROIs is not solved in a general sense, and is attributed to further research. Metabolic processes studied by PET are quantified traditionally using compartmental models, which relate the time course of the tracer concentration in tissue to that in arterial blood. A prerequisite for the quantitative calculation of the tracer kinetics and the biochemical parameters in PET is the availability of the arterial input function, which is difficult to derive from small animal studies due to the limited blood volume in mice and rats. There are several methods proposed to obtain the arterial input function by using direct arterial blood sampling, venous blood sampling or reference tissue models (Chen et al., 2004a; Lammertsma and Hume, 1996; Pain et al., 2004; Wu et al., 1996). On the other hand, non-invasive, image-derived input functions are desirable for quantifying biological functions in dynamic PET studies, but the input functions generated in this way need to be validated (Iida et al., 1992; Huang et al., 2004). However, the measurement of the blood or plasma activity also has to be corrected for possible radioactive metabolites. The possible practical approaches to determine the amount of the parent compound in arterial blood samples has been discussed elsewhere (Pawelke, 2005).

3 PET tracers relevant in food sciences

In general, the production, logistics, and application of PET radiotracers differ from procedures used for conventional drugs in a number of aspects as described in detail by Wuest (2005). The main differences are *a*) because of the short physical half-lives of PET radioisotopes, prolonged preparation time significantly reduces the useful application of the animal PET drug products, *b*) a PET facility usually produces PET drug products in response to daily demand, and *c*) PET radiopharmaceuticals must be administered to the animals shortly after production. Only one or a few lots are produced per day, with one lot equalling to multiple dose vials, allowing, however, only a relatively small number of experiments. An entire lot may be administered in one or in several animals and used in biochemical experiments *in vitro*, depending on the amount and concentration of radioactivity remaining at the time of administration. Consequently, administration of the entire quantity of a lot in the experiments should be anticipated for every lot prepared. Since each multiple-dose vial contains a homogeneous solution of a PET drug product and equals one lot, results from

end-product testing of samples drawn from the vial might be representative not only for the entire lot but for all doses. The quantities of active ingredients in each lot of a PET tracer compound generally vary from microgram to nanogram amounts. PET drug distribution to other PET centres may be applicable when geographic proximity allows distribution with respect to the PET tracer's half-live.

Biodistribution studies in small animals using PET tracers with relevance for food sciences like amino acids have a long history. Only as an example, in studies with selenium-75 labelled methionine all phases of the distribution and metabolism of this essential amino acid in animals have been characterized (Archimbaud et al., 1993; Bergmann et al., 1995; Chen and Wang, 1969; Schultze et al., 1960; Spencer and Blau, 1962). Dynamic PET studies, on the other hand, provide the possibility to image and to measure the flow of the radiotracer through several compartments of the living organism. In this way, many different radiotracers were studied using small animal PET, comprising classes of chemical compounds that are also of interest in food sciences, such as amino acids, peptides, polyamines, lipids, proteins and lipoproteins. The studied PET tracers are either food components itself or analogues that could be used as a surrogate. In other experiments food ingredients were applied as competitive inhibitors of transport or metabolic processes in relation to the PET tracers used. The following overview of substances used as PET tracers in animal PET studies shall emphasise the high potential of the PET methodology.

Amino acids

Radiolabelled amino acids for PET have been widely used in investigations aiming at differences in both amino acid transport and protein synthesis rate in tissues studied (Couturier et al., 2004; Foster and Fagg, 1984; Jager et al., 2001; Laverman et al., 2002; Vaalburg et al., 1992; Wang et al., 2005). An important motivation to study amino acid metabolism *in vivo* is the identification of tumours with increased protein synthesis rate and higher amino acid demand when compared to other tissues. Of these two mechanisms the former is likely to be the most important as regards PET imaging of tumours using radiolabelled amino acids and analogues. The concentration in tumour is, however, limited by efflux of the tracer or its labelled metabolites. This phenomenon may be minimised by choosing non-metabolisable compounds, without any efflux of labelled metabolites or with an efflux which is highly restricted. In addition, these tracers appear to be more specific for tumours than FDG, as protein metabolism in inflammatory cells appears to be less modified than glucose metabolism. Most studies and applications were performed using ^{11}C-labelled amino acids or amino acid derivatives. The most prominent example is ^{11}C-labelled methionine. However, the short physical half-life of ^{11}C prevents its use in most nuclear medicine departments (i.e. those without an on-site cyclotron). Moreover, the physical half-life of ^{11}C is also very short with regard to imaging protein synthesis, which is a fairly long biological process. Radiolabelling of amino acids with ^{18}F, therefore, has gained great interest (Couturier et al., 2004; Laverman et al., 2002). Among the numerous ^{18}F labelled amino acid derivatives that are currently being investigated, tyrosine derivatives have been under particular scrutiny (Table 2).

Peptides

Peptide transporters on epithelia play an important role in the absorption of small peptides and peptide-like drugs. The peptide transporters are in the focus of research for many years. However, the number of PET studies in this field is still limited. To investigate the localization and function of the peptide transporters *in vivo*, peptides, like glycylsarcosine and derivatives were predominantly labelled with ^{11}C (Bolster et al., 1986; Del Rosario et al., 1993; Henriksen et al., 2004; Nabulsi et al., 2005; van Nispen et al., 1990). On the other hand, various peptide receptor ligands, such as peptide hormones were labelled with various longer lived PET radionuclides, e.g., fluorine-18 and copper-64, and used for imaging of tissues, in particular, tumours that overexpress the corresponding peptide hormone receptors (Breeman et al., 2005; Li and Beheshti, 2005; Lundquist and Tolmachev, 2002; Maecke et al., 2005; Reubi, 2003; Reubi et al., 2005; Riccabona and Decristoforo, 2003; Sundin et al., 2004; Virgolini et al., 2005). These include *a*) somatostatin receptor ligands (Anderson et al., 1995; Bass et al., 2000; Bombardieri et al., 2001; Eriksson et al., 1993; Ginj et al., 2005; Guhlke et al., 1994; Lewis et al., 1999; Li and Beheshti, 2005; Pauwels et al., 2005; Robbins, 1996; Schottelius et al., 2004; Sundin et al., 2004; Ugur et al., 2002; Wester et al., 2003; Wild et al., 2005), *b*) gastrin receptor ligands/gastrin-releasing peptide receptor ligands (bombesin receptor ligands) (Chen et al., 2004b; Maina et al., 2005; Meyer et al., 2004; Rogers et al., 2003; Schuhmacher et al., 2005; Zhang et al., 2004), *c*) neurotensin (Achilefu et al., 2003; Bergmann et al., 2002;

Table 2. PET studies with amino acids and analogues

Amino acid	Radiolabelled compound	Reference
Non-essential amino acids and derivatives		
Alanine	α-[2-^{11}C]aminoisobutyric acid	Oberdorfer et al., 1993; Prenant et al., 1995
	α-(*N*-methyl)-[2-^{11}C]aminoisobutyric acid	
Glutamate	[^{13}N]glutamate	Krivokapich et al., 1987; Kubota et al., 1983; Wu et al., 2000b
Glutamine	[^{11}C]glutamate	Wu et al., 2000b
Glycine	[^{11}C]glycine	Bolster et al., 1986
Aspartate	[^{11}C]aspartate	Wu et al., 2000b
Tyrosine	D,L-[1-^{11}C]tyrosine	Daemen et al., 1992, 1991; Halldin et al., 1987
No example: Arginine, Asparagine, Cysteine, Serine		
Essential amino acids		
Leucine	L-[1-^{11}C]leucine	Barrio et al., 1983b; Hawkins et al., 1989; Schmidt et al., 2005
Methionine	Methyl-[^{11}C]-L-methionine	Kubota et al., 1996; Comar et al., 1976; d'Argy et al., 1988; Weber et al., 2000
Phenylalanine	L-[1-^{11}C]phenylalanine	Barrio et al., 1983a; Studenov et al., 2003
Tryptophan	[^{11}C]-D,L-tryptophan	Washburn et al., 1977
Valine	D,L-[^{11}C]valine	Hubner et al., 1979; Washburn et al., 1982
No example: Histidine, Isoleucine, Lysine, Threonine		
Non-natural amino acids and inhibitors of amino acid transport and metabolism		
	O-2-[^{18}F]fluoroethyl-L-tyrosine (l-[^{18}F]FET)	Wang et al., 2005; DeJesus et al., 1992; Hayase et al., 1995; Ishiwata et al., 2005; Iwata et al., 2003; Moon et al., 2005; Tang et al., 2003; Wester et al., 1997, 1999
	L-[2-^{18}F]fluorotyrosine	Coenen et al., 1989
	4-[^{18}F]fluoro-L-*m*-tyrosine	Melega et al., 1989
	4-cis-[^{18}F]fluoro-L-proline	Borner et al., 2001; Langen et al., 2001
	3-[^{18}F]fluoro-α-fluoromethyl-*p*-tyrosine (3-F-FMPT)	DeJesus et al., 1994
	4-Borono-2-[^{18}F]fluoro-D,L-phenylalanine	Ishiwata et al., 1991
	4-Borono-2-[^{18}F]fluoro-l-phenylalanine-fructose (l-[^{18}F]FBPA-Fr)	Chen et al., 2004b
	L-*o*-[^{18}F]fluorophenylalanine	Bodsch et al., 1988
	L-*p*-[^{18}F]fluorophenylalanine	
	L-[β-^{11}C]-3,4-dihydroxyphenylalanine (L-[β-^{11}C]DOPA)	Reiffers et al., 1977; Ikemoto et al., 1999
	L-[β-^{11}C]-5-hydroxytryptophan (L-[β-^{11}C]-5-HTP)	
	3-*O*-methyl-6-[^{18}F]fluoro-L-DOPA (OMFD)	Bergmann et al., 2004; Doudet et al., 1991
	6-[^{18}F]fluoro-L-DOPA (6-[^{18}F]FDOPA)	Ishiwata et al., 1996
	6-[^{18}F]-fluoro-*O*-pivaloyl-L-DOPA (6-[^{18}F]FPDOPA)	
	L-[^{18}F]-2-fluoro-DOPA (L-2-^{18}F-DOPA)	Leenders et al., 1986; Cumming et al., 1988
	L-[^{18}F]-6-fluoro-DOPA (L-6-^{18}F-DOPA)	
	5-hydroxy-L-[β-^{11}C]tryptophan (HTP)	Bergstrom et al., 1996
	2-Amino-3-[^{18}F]fluoro-2-methylpropanoic acid (FAMP)	McConathy et al., 2002
	3-[^{18}F]fluoro-2-methyl-2-(methylamino)propanoic acid (N-MeFAMP)	McConathy et al., 2002
	[^{18}F]-1-amino-3-fluorocyclopentane-1-carboxylic acid (FACPC)	Shoup et al., 1997
	1-aminocyclobutane-[^{11}C]carboxylic acid	Hubner et al., 1981
	1-aminocyclopentane-[^{11}C]carboxylic acid	
	Syn- and *anti*-1-amino-3-[^{18}F]fluoromethyl-cyclobutane-1-carboxylic acid (FMACBC)	Martarello et al., 2002

Bruehlmeier et al., 2002; Buchegger et al., 2003; Garcia-Garayoa et al., 2002), *d*) neurokinin receptor ligands, like substance P (Hargreaves, 2002; Solin et al., 2004), *e*) cholecystokinin (Aloj et al., 2004, 2002; Behe and Behr, 2002; Behr et al., 1999), *f*) vasoactive intestinal peptide (VIP) and pituitary adenylate cyclase-activating peptide (PACAP) (Jagoda et al., 2002; Thakur et al., 2004), and *g*) endothelin (Johnstrom et al., 2002).

Proteins and antibodies

Radiolabelled proteins used in PET investigations comprise a heterogeneous group of compounds that is characterised by a relative high molecular weigth (10–550 kDa). In contrast to most low molecular weight tracers, the biodistribution of protein tracers is governed by the biological characteristics of the protein itself. The presented examples cover some major applications of radiolabelled proteins in PET studies, majority radiolabelled by using ^{18}F-containing prosthetic groups (Wuest, 2005). In this way several proteins have been used as PET tracers, including *a*) human serum albumin that, considering its high biological half life in plasma, was used for imaging of plasma pool, cerebral blood flow, cerebral plasma volume and myocardial perfusion (Okazawa et al., 1995), *b*) Annexin V, a 36-kDa protein that binds with high affinity to phosphatidylserine lipids in the cell membrane and has proven for early imaging (detection) of apoptosis (Grierson et al., 2004; Keen et al., 2005; Murakami et al., 2004; Toretsky et al., 2004; Yagle et al., 2005; Zijlstra et al., 2003), and *c*) antibodies, antibody fragments, antibody minibodies, diabodies, multiple antibody fragment constructs and derivatives that are recognized as promising vehicles for delivery of imaging and therapeutic radionuclides to a wide range of target structures, including tumours *in vivo* (Anderson et al., 1992; Bakir et al., 1992; Collingridge et al., 2002; Griffiths et al., 2004; Keen et al., 2005; Kenanova et al., 2005; Larson et al., 1992; Lovqvist et al., 1997; Olafsen et al., 2004; Otsuka et al., 1991; Pentlow et al., 1991; Robinson et al., 2005; Sundaresan et al., 2003; Verel et al., 2003; Yang et al., 2005; Wu et al., 2000a).

Lipoproteins

Lipoproteins are particles that contribute to overall metabolic homeostasis by transporting hydrophobic lipids and other hydrophobic substances like vitamins and polyphenols in the blood plasma to and from different tissues in the body. Disturbances in lipoprotein metabolism are closely related to various pathophysiologic processes, particularly, in atherogenesis. PET studies using radiolabelled lipoprotein particles aimed at noninvasive delineation of accumulation and tissue metabolism of native lipoproteins under normal and pathophysiologic conditions (Daugherty et al., 1992; Moerlein et al., 1991). More recently, small animal PET has been used to characterize and to discriminate the kinetics and the metabolic fate of native and oxidatively modified lipoproteins (Pietzsch et al., 2004, 2005a, b). These investigations should also provide information about localization, transport, and metabolism as well as about pathways of detoxification of lipid-soluble food ingredients *in vivo*.

Fatty acids and lipids

Lipids comprise a complex family of biomolecules that play prominent roles in critical metabolic and biochemical processes such as energy production and storage, structure and function of cellular membranes, signal transduction, and steroidogenesis. However, lipids and lipid analogues labelled with PET nuclides were mainly used to monitor fatty acid kinetics and tissue uptake as well as lipid metabolism in various tissues. Various ^{11}C- and ^{18}F-labelled fatty acids were applied to animal PET studies (Brown et al., 1987; Buckman et al., 1994; DeGrado et al., 1991, 2000; Geltman, 1994; Geltman et al., 1980; Shoup et al., 2005; Takahashi et al., 1996; Takala et al., 2002).

Fatty acids are the primary metabolic fuel for the myocardium, and, therefore, fatty acid tracers like ^{11}C-acetate, which can be considered as the shortest fatty acid, and ^{11}C-palmitate are very useful in assessing the metabolic status of the heart. This includes measurement of heart perfusion and oxidative metabolism, respectively (Armbrecht et al., 1990; Bentourkia et al., 2002; Brown et al., 1987; Buxton et al., 1989; Go et al., 1990; Higashi et al., 2004; Liu et al., 2001; Ng et al., 1994; Oyama et al., 2002, 2003; Prenen et al., 1989; Rasmussen et al., 2004; Schelbert, 2000; Schoder and Larson, 2004; Shoup et al., 2005; Sun et al., 1997; Visser, 2001; Yoshimoto et al., 2001). Other intravenously injected fatty acids like ^{11}C-arachidonic acid were used to quantify uptake of polyunsaturated fatty acids into brain tissue, to quantitatively localize brain phospholipase A_2-mediated signal transduction, and to examine neuroplastic remodeling of brain lipid membranes *in vivo* (Rapoport, 2001).

Oligonucleotides and related molecules

On the basis of oligonucleotides or related molecules, such as antisense DNA or iRNA molecules, aptamers, spiegelmers or ribozymes as well as peptide nucleic acids, several PET tracer compounds became available as imaging agents for the detection of specific target molecules (Berger and Gambhir, 2001; Boisgard et al., 2005; de Vries et al., 2004; Duatti, 2004; Eschgfaller et al., 1998; Kobori et al., 1999; Kuhnast et al., 2005; Lange et al., 2002; Lendvai et al., 2005; Pan et al., 1998; Pestourie et al., 2005; Roivainen

et al., 2004; Sun et al., 2005; Tavitian et al., 2002; Tavitian, 2003; Wu et al., 2000c; Younes et al., 2002).

Nucleotides and nucleotide analogues

Nucleotides, nucleotide analogues and structure related compounds were developed for the investigation of nucleotide incorporation into nucleic acids. When the agents undergo phosphorylation in the cells the resulting tissue accumulation of radioactivity may provide specific information on tissue proliferation in diagnostic imaging and therapy monitoring. Prominent examples are 3′-deoxy-3′-[^{18}F]fluorothymidine and, 5-[^{18}F]-2′-deoxyuridine and (Barthel et al., 2005; Seitz et al., 2001). Another group of nucleotides and nucleotide analogues like 2′-deoxy-2′-^{18}F-fluoro-5-fluoro-1-beta-D-arabinofuranosyluracil, 9-(4-^{18}F-fluoro-3-hydroxymethylbutyl)guanine, 8-[^{18}F]fluoropenciclovir, and 8-[^{18}F]fluoroganciclovir has been synthesized and tested for monitoring the expression of herpes simplex virus type 1 thymidine kinase reporter gene in cell culture and *in vivo* (Alauddin et al., 2004; Iyer et al., 2001). Very recently, it could demonstrated that ^{124}I-labelled 2′-fluoro-2′-deoxy-5′-iodo-1-beta-D-arabinofuranosyluracil is suitable for PET of myocardial expression of herpes simplex virus type 1 thymidine kinase reporter gene (Simoes et al., 2005).

Drugs

The unique possibility to visualize and quantify metabolic routes of radiolabelled drugs *in vivo* enormously accelerated the application of small animal PET in the last years (Aboagye, 2005; Myers, 2001; Paans and Vaalburg, 2000; Roselt et al., 2004; Vaalburg et al., 1999). As an example, 8-cyclopentyl-3-(3-^{18}F-fluoropropyl)-1-propylxanthine (^{18}F-CPFPX) was developed as a highly selective and specific ligand for adenosine receptors and a suitable radioligand for non-invasive PET imaging of adenosine receptors in the living brain. These studies also support the application of high-resolution animal PET as an effective *in vivo* imaging tool in the evaluation process of new radioligands (Bauer et al., 2003, 2005).

Trace elements

The vast number of positron emitting nuclides that are suitable for PET studies comprise also isotopes of micronutrients (Anderson and Welch, 1999). For instance, by using the copper isotope ^{64}Cu ($t_{1/2} = 12.70$ h) the whole body copper flux was measured by PET. After oral administration, the copper was trapped in the gastrointestinal tract. This trapping does, however, limit the utility of PET to completely measure the whole animal copper flux (Bissig et al., 2005).

The manganese isotope ^{52m}Mn ($t_{1/2} = 21.10$ h) can be produced in a ^{52}Fe/^{52m}Mn generator. It is a suitable radionuclide to quantitatively assess myocardial perfusion (Buck et al., 1996). Animal studies indicate that ^{52m}Mn is an ideal nuclide for myocardial imaging, combining rapid blood clearance and high concentration in the myocardium (Atcher et al., 1980). The PET nuclides of cobalt, iron and gallium, ^{55}Co ($t_{1/2} = 17.53$ h), ^{52}Fe ($t_{1/2} = 8.28$ h), ^{66}Ga ($t_{1/2} = 9.49$ h), and ^{68}Ga ($t_{1/2} = 1.13$ h) were applied for blood cell labelling to enable quantitative uptake and cell kinetic studies in rats. Furthermore, these radionuclides have been used kidney function imaging, cisternography, and bleomycin labeling (Ellis and Sharma, 1999; Goethals et al., 2000; Maziere et al., 1983; Sharma et al., 1986). In principle, the iodine PET isotope ^{124}I ($t_{1/2} = 4.2$ days) can be applied for the same indications as ^{123}I and ^{131}I that are commonly used in biomedical research and clinical practice, like diagnostic imaging of the thyroid function as well as diagnosis of abnormal liver function, renal (kidney) blood flow and urinary tract obstruction (Collingridge et al., 2002; Crawford et al., 1997; Eschmann et al., 2002; Flower et al., 1994; Freudenberg et al., 2003; Groot-Wassink et al., 2004; Klein et al., 2005; Larson et al., 1992; Sundaresan et al., 2003; Verel et al., 2003). However, ^{124}I became important as a peptide and protein labelling agent for PET studies (Collingridge et al., 2002; Daghighian et al., 1993; Dekker et al., 2005; Pentlow et al., 1996; Robinson et al., 2005; Shaul et al., 2004). The biodistribution and metabolism of the single photon emitting isotope ^{75}Se was intensively studied in the past (Archimbaud et al., 1993; Bawden and Hammarstrom, 1977; Bergmann et al., 1995; Jalilian et al., 2004; Jian et al., 1982; McConnell, 1959; McConnell and Roth, 1968; Nahapetian et al., 1983; Wright, 1965). However, there is only a very limited number of PET studies using ^{73}Se ($t_{1/2} = 7.15$ h). The very sophisticated production of ^{73}Se and the dosimetric characteristics are the main limitations for a broader application of ^{73}Se in PET (Plenevaux et al., 1990). The vanadium isotope ^{48}V ($t_{1/2} = 16$ days) has been used as a tracer to investigate tissue distributions of bis(maltolato) oxovanadium(IV) compared with those of vanadyl sulfate in Wistar rats. In this study, the compounds were administered in carrier-added forms by either oral gavage or intraperitoneal injection. The highest ^{48}V concentrations at 24 h after gavage were found in bone, followed by kidney and liver. Most ^{48}V ingested was eliminated unabsorbed by fecal excretion. On average, ^{48}V concentrations in bone, kidney, and liver 24 h after oral administration of

bis(maltolato)oxo-[^{48}V]vanadium(IV) were two to three times higher than those of ^{48}V-vanadyl sulfate (Setyawati et al., 1998). As zinc is closely associated with the exocrine and endocrine functions of the pancreas, exploitation of zinc metabolism for anatomical and functional diagnosis was conceived, namely with the recently available of positron emitting isotope ^{62}Zn ($t_{1/2} = 9.19$ h). The response changes in Zn biodistribution (mice) and Zn excretion through the pancreatic duct (rats) due to the stimulation of gastrointestinal hormones, like secretin, by cholecystokin-pancreozymin (exocrine stimulation) and glucose (endocrine stimulation) were studied. Demonstration of zinc participation in the exocrine function of the pancreas *in vivo* holds considerable promise for diagnosis of pancreatic diseases (Fujibayashi et al., 1986). Fluorine-18, as one of the most important PET nuclides, has been used as fluoride ($^{18}F^-$) for imaging of bone metabolism (Piert et al., 2003, 2001; Hoegerle et al., 1998; Hawkins et al., 1992). Very recently, the titanium isotope ^{45}Ti ($t_{1/2} = 3.09$ h) was prepared as a tool for elucidation of the mechanism of action of titanium anticancer drugs *in vivo* using small animal PET imaging (Vavere et al., 2005).

Plant secondary metabolites

There are many different types of plant secondary metabolites such as plant hormones, phenolic compounds, vitamins, alkaloids etc. Plants produce secondary metabolites as chemical defence against fungi, bacteria, insects, and viruses. The potential use of plant secondary metabolites in medicine as diagnostic and therapeutic agents, and in agriculture as biorational pesticides is of increasing interest. In this line, ^{11}C-colchicine has been used in studies aiming at evaluation of multiple drug resistance by PET imaging (Levchenko et al., 2000). As another example, polyphenols, such as stilbenes and flavonoids have attracted attention as foodborne antioxidants or estrogen receptor ligands with many different implications in human metabolism (Middleton et al., 2000). A first approach for radiosynthesis of an ^{18}F-labelled stilbene derivative (3,5-dihydroxy-4′-[^{18}F]fluoro-*trans*-stilbene) and subsequent radiopharmacological investigation including dynamic PET studies in rats has been described in this isssue (Gester et al., 2005).

Vitamins and vitamin derivatives

Radiolabelled biotin and biotin derivatives play a central role in the application of the biotin/avidin pretargeting system of PET tracers and, additionally, also in other applications, like infection imaging (Lewis et al., 2002, 2003; Shoup et al., 1994). The vitamin D receptor ligend [26,27-^{11}C]dihydroxyvitamin D_3 was developed as a potential tracer for PET determination of vitamin D receptor level and occupancy in animals *in vivo* (Bonasera et al., 2001). An example of another vitamin derivative is the folate-receptor-targeting radiopharmaceutical, Ga(III)-deferoxamine-folate, which was radiolabelled with two positron-emitting isotopes of gallium, cyclotron-produced ^{66}Ga and generator-produced ^{68}Ga. The [^{66}Ga]-Ga-deferoxamine-folate was administered to athymic mice with folate-receptor-positive human KB cell tumor xenografts to demonstrate that small animal PET mouse tumor imaging is feasible with ^{66}Ga, despite the relatively high positron energy of this radionuclide (Mathias et al., 2003).

Carbohydrates

The most prominent carbohydrate tracer in PET with the most applications and the longest history in use is the glucose analogue 2-[^{18}F]fluoro-2-deoxy-D-glucose (FDG) (Jones et al., 1983; Phelps et al., 1979; Wolf and Redvanly, 1977). There are practical no research fields in PET, except for perfusion, where the FDG distribution and uptake does not play the role as golden standard or as reference for the metabolic activity of the tissue of interest (Fowler and Ido, 2002; Smith, 1998; Wang et al., 2005; Yamamoto et al., 2004).

4 Small animal PET to measure food uptake, distribution and metabolism *in vivo*: limitations and implications

As outlined above, PET technology now has been implemented in experiments with small laboratory animals. It can be used for serial assessment of metabolic function of individual animals with a minimal degree of invasiveness and, therefore, has the potential to be used in studies of variable physiological and pathophysiological conditions (Kornblum et al., 2000). This should also include conditions that are relevant for food sciences, e.g., in variable nutrition states. However, small animal PET requires the control of the current physiological state of the animals, like body temperature, respiration, and blood pressure. A further important problem is the movement control in order to prevent artefacts in the PET images (Green et al., 2001). For this reason, animals must be either physically restrained or anesthetized. Movement correction of measured data is under development in human studies, however, yet to be developed for small animals (Buhler et al., 2004). The choice of the applied method for minimization of movement depends on the physiological or

biochemical process to be studied, on the localization of the tissue of interest, and on the used radiotracer. The anaesthesia, for example, has significant effects on the central nervous, cardiovascular and respiratory systems (Croteau et al., 2004; Shimoji et al., 2004; Toyama et al., 2004). Further sources of possible movement effects are organ specific movements of the heart, the respiration system, and the intestine. The periodical movements like heart beat or breathing movements were used for gating of the PET imaging (Croteau et al., 2003; Susskind et al., 1985). This shows that it is necessary to control and characterize the experimental conditions, which could affect the uptake, accumulation, metabolism, and elimination of the radiotracer.

An important limitation of PET is the short half-lives of the commonly used PET isotopes in relation to many biological processes. Therefore, the PET study duration typically should not exceed two to four times of the half-life of the PET isotope used to get a low noise and an accurate statistics of the measurement. Consequently, the rate-limiting step of the biochemical or molecular process studied has to be within the time window available. As in other approaches, the resulting radiopharmaceutical distribution and kinetics depend on the route and the duration of radiotracer administration into the animals (Fig. 1). Therefore, it is necessary to minimize the time for uptake and distribution of the radiopharmaceuticals in the body. Therefore, the intravenous application of the radiopharmaceuticals is by far the most preferred administration route. The pharmaceuticals can be applied either as bolus, e.g., as a short impulse, or as an infusion. The transition

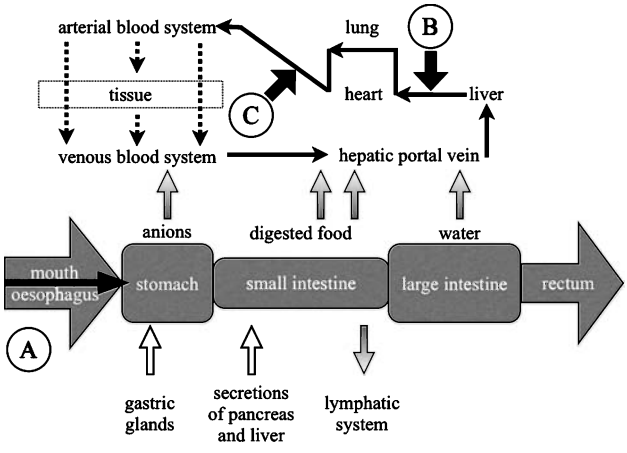

Fig. 1. Routes of administration of radiopharmaceuticals in small animal PET studies and ways of main uptake and elimination, respectively. (**A**) trans-gastrointestinal administration, (**B**) intravenous administration, (**C**) intraarterial administration

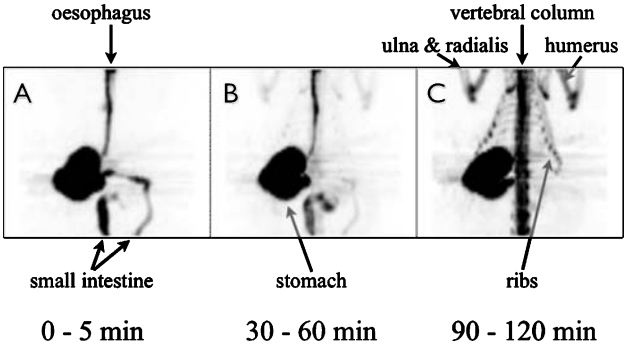

Fig. 2. Representative serial coronal images of abdominal region obtained from dynamic small animal PET scans showing [^{18}F]-radioactivity distribution after administration of [^{18}F]fluoride into the stomach by gavage in rat. The measurements were carried out with microPET P4 (CTI Concorde Microsystems, USA) through 2 hours after application. The data for the images were collected from 0 to 5 min (**A**), 30 to 60 min (**B**), and 90–120 min (**C**). Selected planes illustrate that the radioactivity leaving the stomach was fast absorbed from the duodenum, and accumulated in the metabolically active skeleton sites, like joints and vertebral bodies

between the application types is fluid. An essential prerequisite for quantitative analysis of pharmacokinetic parameters of a tracer in tissues of interest is the arterial blood activity curve as described elsewhere (van den Hoff, 2005). Some experiments require intra-arterial tracer administration or direct administration of tracer into the capillary bed of an organs, e.g., to study first pass effects of the endothelium (Yudilevich, 1989). These application types result in fast distribution of the radiopharmaceuticals within the blood pool or specific target tissue. In this case, the equilibrium between arterial and venous blood is reached relatively fast, however, still depending on the metabolism of the compound used. Fast absorption of radiopharmaceuticals can be observed following intraperitoneal administration. However, the remaining contamination of the peritoneal region with radiotracer that is not resorbed may decrease the target to background ratio in the abdomen. Other administration routes, like intrathecal application, are practically not used in small animal PET studies (McCarthy et al., 2002). However, for small animal PET studies in food sciences it seems to be of special importance to administer the radiopharmaceutical directly into the stomach. This should be illustrated by two examples obtained in our own laboratory. Figures 2, 3, and 4 illustrate a small animal PET study using ^{18}F-fluoride ($^{18}F^-$) in a rat. The *non-carrier-added* (n.c.a.) $^{18}F^-$ was administered by gavage. The radioactivity in the stomach decreased only slowly. It is supposed that $^{18}F^-$ was slowly taken up from stomach, and with higher efficiency from the duodenum (Whitford and Pashley, 1984). The activity

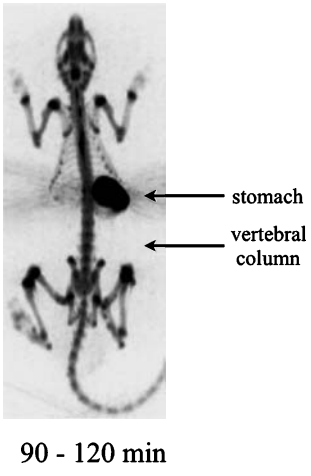

Fig. 3. Representative whole-body coronal image obtained from small animal PET scans showing distribution of [^{18}F]fluoride in rat after administration into the stomach by gavage. The measurements were carried out with microPET P4 (CTI Concorde Microsystems, USA) through 2 hours after application. The data were collected from 90–120 min. The activity was located in the stomach and in the metabolically active skeleton sites, like joints, and vertebral bodies

in the duodenum was scarcely visible during the study. The $^{18}F^-$ was than accumulated in the highly perfused and metabolic active parts of the skeleton (Berger et al., 2002; Piert et al., 2001). The quantitative evaluation of the $^{18}F^-$ distribution was carried out in the stomach and the vertebral bodies. As shown in Fig. 4, during the study time most radioactivity remains in the stomach. However, the activity in the vertebral bodies increased continuously over the time of two hours, which was longer than in studies using an intravenous application of the radiotracer (Berger et al., 2002). In this pioneering study the stomach has been identified as a high capacity source of $^{18}F^-$ over the time studied. In the second example FDG was used to demonstrate the effect of specific activity of a radiopharmaceutical used in small animal PET studies to be a key parameter for such experiments (Figs. 5 and 6). With increasing amounts of glucose, the absorption of FDG in the gastrointestinal tract decreased when compared to n.c.a. conditions. By variation of the effective specific activity of FDG, it should be possible to measure the uptake dependent on the radiotracer concentration and to calculate apparent kinetic parameters, like the Michaelis-Menten constant and the maximal transport rate in the intestine. However, when using a direct administration of the tracer via the gastrointestinal tract, tracer binding, uptake and metabolization influenced by the microflora has to be considered. After intestinal absorption the hepatic first-pass metabolism plays a key role in metabolic regulation and drug metabolism. A first PET approach to measure hepatic first-pass metabolism of ammonia was developed by Keiding and colleagues (Keiding et al., 2001). In this study, pigs were administered $^{13}NH_3$ into the portal vein and into the vena cava. Vena cava infusion data were used to address recirculation of the tracer and metabolites following the portal vein infusion. The data

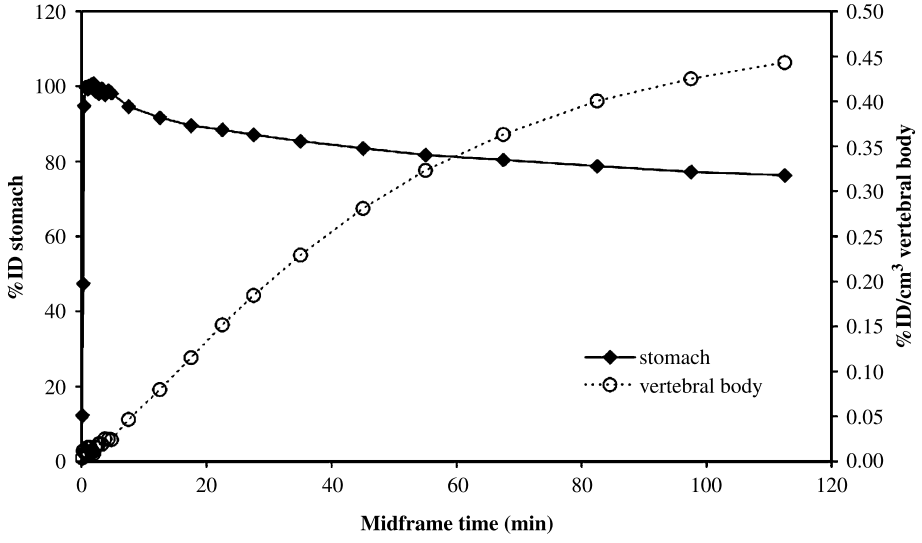

Fig. 4. Time-activity curves showing kinetics of the [^{18}F]-radioactivity concentration during the entire study period of 120 min fluoride after a single administration of [^{18}F]fluoride into the stomach by gavage in the rat after a single administration into the stomach by gavage. Data were calculated from ROI analysis of dynamic small animal PET scans over the stomach and the vertebral bodies. The activity in the stomach is expressed as % injected dose (left y-axis), and the activity in the vertebral bodies is expressed as % injected dose per cm^3 (right y-axis). The activity was continually accumulated in the vertebral bodies

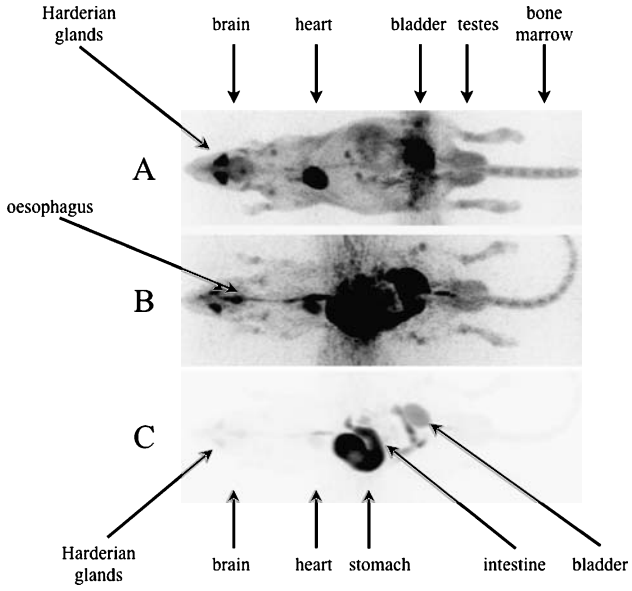

Fig. 5. Comparison of [^{18}F]-radioactivity distribution after intravenous administration (**A**) and administration by gavage (**B**, **C**), respectively, of FDG in rat. The measurements were carried out with microPET P4 (CTI Concorde Microsystems, USA) at 45 min after application. The gray scale of the images (**A**) and (**C**) are normalized to the maximal activity, where white is low and black is high activity. The image (**B**) shows the the same experiment as (**C**), but the gray scale has been changed, so that the details with mean activity (gray) are comparable to image (**A**). The images (**A**) and (**B**) illustrate that the main difference between the two application routes consists in the remaining activity in the stomach and intestinum after gavage, which is to see in detail in the image (**C**). The distribution of FDG in the other organs after intravenous application or after the uptake into the blood, was comparable. As expected, the best-imaged organs were bladder, the heart, the Harderian glands, the brain, the testes, and red bone marrow

were analysed by a model of sinusoidal zonation of ammonia metabolism with periportal urea formation and perivenous formation of glutamine. The hepatic extraction fraction and values of clearance of ammonia to urea and to glutamine were obtained, as were rate constants for washout of these two metabolites (Keiding et al., 2001).

Other important factors influencing the biodistribution of the PET tracers are dependent on the species, the gender, the age, and the actual feeding and satiety situation (de Graaf et al., 2004; Stephan et al., 2003; Gautier et al., 2000; Geary et al., 1982). Animal studies have provided some convincing evidence that nutritional factors *in utero* and in infancy can effectively cause long term changes in metabolism and physiology, but the cellular and molecular mechanisms involved are still largely unknown. Small animal PET allows follow up studies in the individual development of the metabolism, e.g., glucose metabolism, from infancy to the old age. Developmental changes were studied in amino acid and neurotransmitter metabolism (Bauer et al., 2002, 2000; Brust et al., 1999, 1998, 2004a, b). There are only few PET studies aiming at metabolic sex differences of biodistribution and elimination kinetics of the radiotracers (Colby and Morenko, 2004; Zubieta et al., 1999). These data imply that both age and gender are important variables to be considered in the interpretation of studies of the measured function in which receptor systems play a role. Also in animal experiments, the females' reproductive status (reproductive

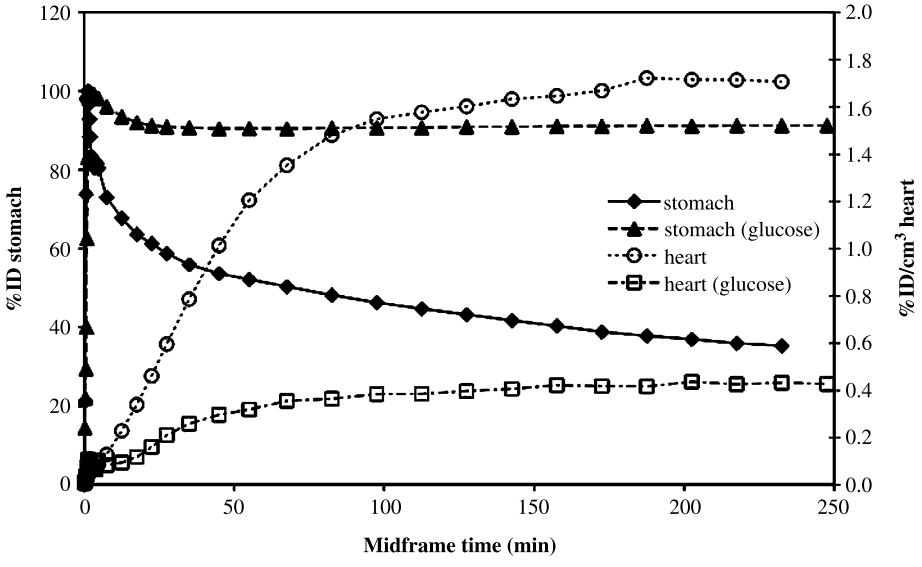

Fig. 6. Comparison of the kinetics of the FDG in in the stomach and heart after administration by gavage into the stomach without and with concomitant admistration of 0.2 g glucose (signed as glucose). The measurements were carried out with microPET P4 (CTI Concorde Microsystems, USA) over 4 hours after application. Time-activity curves were calculated from ROI analysis of dynamic small animal PET scans over the heart (mainly representing the cardiac blood pool) and the stomach. The activity is expressed as % injected dose in the stomach (left y-axis) and % injected dose per cm^3 in the heart (right y-axis). The elimination of FDG from the stomach and accumulation in the heart were faster without addition of glucose. The absolute uptake of FDG in the heart was also increased in this case

age) may influence the function of endocrine receptor systems. On the other hand, the experimental conditions have also an influence on the physiological and metabolic state of the studied animals (Mitterhauser et al., 2003). The protocol of aesthesia, the used drug and the time of start, are among the important experimental factors influencing the quantification (Croteau et al., 2004; Duffy et al., 1982; Matsumura et al., 2003; Momosaki et al., 2004; Nader et al., 1999; Noda et al., 2003; Toyama et al., 2004). Many radiotracers are substrates of endogenous enzymes and are metabolised (Bauer et al., 2002; Lecomte, 2004; Kates et al., 2003; Noda et al., 2002). The radioactive signal measured by PET therefore consists of the original compound and its radioactive metabolites. The tissues of interest have to be analysed for the composition of the radioactive signal in relation to the original compound (Pawelke, 2005). This is often accomplished by homogenisation of the sample, precipitation, and followed by radiochromatographic analysis methods (high performance liquid chromatography, thin layer chromatography). High molecular weight compounds were studied by size-exclusion chromatography and electrophoresis. The radioanalytical methods should especially be optimized in terms of short analysis times with respect to the short-lived radioisotopes used. The number of samples to be analysed should also be taken into account by the selection of analytical methods. When the arterial time activity curves for free intact tracer and metabolites have to be determined for compartmental modelling, then only the largest number of analysed samples seems to be good enough. In the case that metabolites share the same compartment together with the intact compound it is necessary to analyse the tissues of interest at sufficient time points for validation purposes. The non-invasive PET method moves to an invasive one. Furthermore, pharmacokinetic PET studies could be combined with microdialysis measurements in the tissues of interest to get samples of the interstitial fluid (Haaparanta et al., 2004).

5 Conclusion

As discussed above small animal PET has a high potential to depict physiologic processes like absorption, distribution, metabolism, elimination and interactions of biologically significant substances, including nutrients, 'nutriceuticals', functional food ingredients, and foodborne toxicants, *in vivo*. Thus, among nuclear and isotope techniques small animal PET is supposed to be an attractive tool to endorse to and to expand the classical pharmacokinetic, pharmodynamic and toxicological approaches in food sciences, e.g., in nutritional studies. However, progress can only be achieved when multidisciplinary PET centers closely cooperate with food scientists and food-producing companies. Furthermore, industry and regulators should recognize that the use of functional *in vivo* imaging supports the decision-making whether food components are harmful or, on the other hand, maintain human health.

Acknowledgements

The authors are grateful to Frank Wuest, PhD, for his expert advice and many stimulating discussions. The authors are also grateful to Mrs. Regina Herrlich and Ms. Mareike Barth for their excellent technical assistance in the animal experiments.

References

Aboagye EO (2005) Positron emission tomography imaging of small animals in anticancer drug development. Mol Imaging Biol 7: 53–58

Achilefu S, Srinivasan A, Schmidt MA, Jimenez HN, Bugaj JE, Erion JL (2003) Novel bioactive and stable neurotensin peptide analogues capable of delivering radiopharmaceuticals and molecular beacons to tumors. J Med Chem 46: 3403–3411

Alauddin MM, Shahinian A, Park R, Tohme M, Fissekis JD, Conti PS (2004) Synthesis and evaluation of 2′-deoxy-2′-^{18}F-fluoro-5-fluoro-1-beta-D-arabinofuranosyluracil as a potential PET imaging agent for suicide gene expression. J Nucl Med 45: 2063–2069

Aloj L, Panico MR, Caraco C, Zannetti A, Del Vecchio S, Di Nuzzo C, Arra C, Morelli G, Tesauro D, De Luca S, Pedone C, Salvatore M (2002) Radiolabeling approaches for cholecystokinin B receptor imaging. Biopolymers 66: 370–380

Aloj L, Caraco C, Panico M, Zannetti A, Del Vecchio S, Tesauro D, De Luca S, Arra C, Pedone C, Morelli G, Salvatore M (2004) *In vitro* and *in vivo* evaluation of ^{111}In-DTPAGlu-G-CCK8 for cholecystokinin-B receptor imaging. J Nucl Med 45: 485–494

Anderson CJ, Welch MJ (1999) Radiometal-labeled agents (non-technetium) for diagnostic imaging. Chem Rev 99: 2219–2234

Anderson CJ, Connett JM, Schwarz SW, Rocque PA, Guo LW, Philpott GW, Zinn KR, Meares CF, Welch MJ (1992) Copper-64-labeled antibodies for PET imaging. J Nucl Med 33: 1685–1691

Anderson CJ, Pajeau TS, Edwards WB, Sherman ELC, Rogers BE, Welch MJ (1995) *In-vitro* and *in-vivo* evaluation of copper-64-octreotide conjugates. J Nucl Med 36: 2315–2325

Archimbaud Y, Grillon G, Poncy JL, Masse R (1993) Age-dependent variation of selenium-75 biokinetics in rat. Int J Radiat Biol 64: 329–333

Armbrecht JJ, Buxton DB, Schelbert HR (1990) Validation of [1-^{11}C] acetate as a tracer for noninvasive assessment of oxidative metabolism with positron emission tomography in normal, ischemic, postischemic, and hyperemic canine myocardium. Circulation 81: 1594–1605

Atcher RW, Friedman AM, Huizenga JR, Rayudu GV, Silverstein EA, Turner DA (1980) Manganese-52 m, a new short-lived, generator-produced radionuclide: a potential tracer for positron tomography. J Nucl Med 21: 565–569

Auffray E, Bruyndonckx P, Devroede O, Fedorov A, Heinrichs U, Korjik M, Krieguer M, Kuntner C, Lartizien C, Lecoq P, Leonard S, Morel C, Mosset JB, Pedrini C, Petrosian A, Pietrzyk U, Rey M, Saladino S, Sappey-Marinier D, Simon L, Streun M, Tavernier S, Vieira JM, Ziemons K (2004) The ClearPET project. Nuclear Instruments & Methods in Physics Research Section A – Accelerators, Spectrometers, Detectors and Associated Equipment 527: 171–174

Bakir MA, Eccles S, Babich JW, Aftab N, Styles J, Dean CJ, Lambrecht RM, Ott RJ (1992) c-erbB2 protein overexpression in breast cancer as a target for PET using iodine-124-labeled monoclonal antibodies. J Nucl Med 33: 2154–2160

Barrio JR, Keen R, Chugani H, Ackerman R, Chugani DC, Phelps ME (1983a) L-[1-C-11]phenylalanine for the determination of cerebral protein-synthesis rates in man with positron emission tomography. J Nucl Med 24: P70–P70

Barrio JR, Keen RE, Ropchan JR, MacDonald NS, Baumgartner FJ, Padgett HC, Phelps ME (1983b) L-[1-^{11}C]leucine: routine synthesis by enzymatic resolution. J Nucl Med 24: 515–521

Barthel H, Perumal M, Latigo J, He Q, Brady F, Luthra SK, Price PM, Aboagye EO (2005) The uptake of 3′-deoxy-3′-[^{18}F]fluorothymidine into L5178Y tumours *in vivo* is dependent on thymidine kinase 1 protein levels. Eur J Nucl Med Mol Imaging 32: 257–263

Bass LA, Wang M, Welch MJ, Anderson CJ (2000) *In vivo* transchelation of copper-64 from TETA-octreotide to superoxide dismutase in rat liver. Bioconjug Chem 11: 527–532

Bauer R, Brust P, Walter B, Vorwieger G, Bergmann R, Fuchtner F, Steinbach J, el-Hallag E, Fritz A, Johannsen B, Zwiener U (2000) Relation between brain tissue pO_2 and dopamine synthesis of basal ganglia – a ^{18}FDOPA-PET study in newborn piglets. J Perinat Med 28: 54–60

Bauer R, Brust P, Walter B, Vorwieger G, Bergmann R, Elhalag E, Fritz A, Steinbach J, Fuchtner F, Hinz R, Zwiener U, Johannsen B (2002) Effect of hypoxia/hypercapnia on metabolism of 6-[^{18}F]fluoro-L-DOPA in newborn piglets. Brain Res 934: 23–33

Bauer A, Holschbach MH, Cremer M, Weber S, Boy C, Shah NJ, Olsson RA, Halling H, Coenen HH, Zilles K (2003) Evaluation of ^{18}F-CPFPX, a novel adenosine A1 receptor ligand: *in vitro* autoradiography and high-resolution small animal PET. J Nucl Med 44: 1682–1689

Bauer A, Langen KJ, Bidmon H, Holschbach MH, Weber S, Olsson RA, Coenen HH, Zilles K (2005) ^{18}F-CPFPX PET identifies changes in cerebral A1 adenosine receptor density caused by glioma invasion. J Nucl Med 46: 450–454

Bawden JW, Hammarstrom LE (1977) Autoradiography of selenium-75 in developing rat teeth and bone. Caries Res 11: 195–203

Behe M, Behr TM (2002) Cholecystokinin-B (CCK-B)/gastrin receptor targeting peptides for staging and therapy of medullary thyroid cancer and other CCK-B receptor expressing malignancies. Biopolymers 66: 399–418

Behr TM, Jenner N, Behe M, Angerstein C, Gratz S, Raue F, Becker W (1999) Radiolabeled peptides for targeting cholecystokinin-B/gastrin receptor-expressing tumors. J Nucl Med 40: 1029–1044

Bentourkia M (2003) PET kinetic modeling of ^{11}C-acetate from projections. Comput Med Imaging Graph 27: 373–379

Bentourkia M, Croteau E, Langlois R, Aliaga A, Cadorette J, Benard F, Lesur O, Lecomte R (2002) Cardiac studies in rats with C-11-acetate and PET: a comparison with N-13-ammonia. IEEE Trans Nucl Sci 49: 2322–2327

Berger F, Gambhir SS (2001) Recent advances in imaging endogenous or transferred gene expression utilizing radionuclide technologies in living subjects: applications to breast cancer. Breast Cancer Res 3: 28–35

Berger F, Lee YP, Loening AM, Chatziioannou A, Freedland SJ, Leahy R, Lieberman JR, Belldegrun AS, Sawyers CL, Gambhir SS (2002) Whole-body skeletal imaging in mice utilizing microPET: optimization of reproducibility and applications in animal models of bone disease. Eur J Nucl Med Mol Imaging 29: 1225–1236

Bergmann R, Brust P, Kampf G, Coenen HH, Stocklin G (1995) Evaluation of radioselenium labeled selenomethionine, a potential tracer for brain protein synthesis by PET. Nucl Med Biol 22: 475–481

Bergmann R, Scheunemann M, Heichert C, Mading P, Wittrisch H, Kretzschmar M, Rodig H, Tourwe D, Iterbeke K, Chavatte K, Zips D, Reubi JC, Johannsen B (2002) Biodistribution and catabolism of ^{18}F-labeled neurotensin (8–13) analogs. Nucl Med Biol 29: 61–72

Bergmann R, Pietzsch J, Fuechtner F, Pawelke B, Beuthien-Baumann B, Johannsen B, Kotzerke J (2004) 3-O-methyl-6-^{18}F-fluoro-L-dopa, a new tumor imaging agent: investigation of transport mechanism *in vitro*. J Nucl Med 45: 2116–2122

Bergstrom M, Lu L, Eriksson B, Marques M, Bjurling P, Andersson Y, Langstrom B (1996) Modulation of organ uptake of C-11-labelled 5-hydroxytryptophan. Biogenic Amines 12: 477–485

Bissig KD, Honer M, Zimmermann K, Summer KH, Solioz M (2005) Whole animal copper flux assessed by positron emission tomography in the Long-Evans cinnamon rat – a feasibility study. Biometals 18: 83–88

Bocan TM (1998) Animal models of atherosclerosis and interpretation of drug intervention studies. Curr Pharm Des 4: 37–52

Bodsch W, Coenen HH, Stocklin G, Takahashi K, Hossmann KA (1988) Biochemical and autoradiographic study of cerebral protein synthesis with [^{18}F]- and [^{14}C]fluorophenylalanine. J Neurochem 50: 979–983

Boisgard R, Vincent-Naulleau S, Leplat JJ, Bouet S, Le Chalony C, Tricaud Y, Horak V, Geffrotin C, Frelat G, Tavitian B (2003) A new animal model for the imaging of melanoma: correlation of FDG PET with clinical outcome, macroscopic aspect and histological classification in melanoblastoma-bearing Libechov Minipigs. Eur J Nucl Med Mol Imaging 30: 826–834

Boisgard R, Kuhnast B, Vonhoff S, Younes C, Hinnen F, Verbavatz JM, Rousseau B, Furste JP, Wlotzka B, Dolle F, Klussmann S, Tavitian B (2005) *In vivo* biodistribution and pharmacokinetics of ^{18}F-labelled Spiegelmers: a new class of oligonucleotidic radiopharmaceuticals. Eur J Nucl Med Mol Imaging 32: 470–477

Bolster JM, Vaalburg W, Elsinga PH, Woldring MG, Wynberg H (1986) Synthesis of carbon-11 labelled glycine and the dipeptides L-phenylalanylglycine and L-leucylglycine. Int J Rad Appl Instrum [A] 37: 985–987

Bombardieri E, Maccauro M, De Deckere E, Savelli G, Chiti A (2001) Nuclear medicine imaging of neuroendocrine tumours. Ann Oncol 12 [Suppl 2]: S51–S61

Bonasera TA, Grue-Sorensen G, Ortu G, Binderup E, Bergstrom M, Bjorkling F, Langstrom B (2001) The synthesis of [26,27-^{11}C]dihydroxyvitamin D(3), a tracer for positron emission tomography (PET). Bioorg Med Chem 9: 3123–3128

Borner AR, Langen KJ, Herzog H, Hamacher K, Muller-Mattheis V, Schmitz T, Ackermann R, Coenen HH (2001) Whole-body kinetics and dosimetry of cis-4-[^{18}F]fluoro-L-proline. Nucl Med Biol 28: 287–292

Breeman WA, de Jong M, de Blois E, Bernard BF, Konijnenberg M, Krenning EP (2005) Radiolabelling DOTA-peptides with 68 Ga. Eur J Nucl Med Mol Imaging 32: 478–485

Brown M, Marshall DR, Sobel BE, Bergmann SR (1987) Delineation of myocardial oxygen utilization with carbon-11-labeled acetate. Circulation 76: 687–696

Bruehlmeier M, Garayoa EG, Blanc A, Holzer B, Gergely S, Tourwe D, Schubiger PA, Blauenstein P (2002) Stabilization of neurotensin analogues: effect on peptide catabolism, biodistribution and tumor binding. Nucl Med Biol 29: 321–327

Brust P, Bauer R, Walter B, Bergmann R, Fuchtner F, Vorwieger G, Steinbach J, Johannsen B, Zwiener U (1998) Simultaneous measurement of [^{18}F]FDOPA metabolism and cerebral blood flow in newborn piglets. Int J Dev Neurosci 16: 353–364

Brust P, Bauer R, Vorwieger G, Walter B, Bergmann R, Fuchtner F, Steinbach J, Zwiener U, Johannsen B (1999) Upregulation of the aromatic amino acid decarboxylase under neonatal asphyxia. Neurobiol Dis 6: 131–139

Brust P, Vorwieger G, Walter B, Fuchtner F, Stark H, Kuwabara H, Herzau M, Opfermann T, Steinbach J, Ganapathy V, Bauer R (2004a) The

influx of neutral amino acids into the porcine brain during development: a positron emission tomography study. Brain Res Dev Brain Res 152: 241–253

Brust P, Walter B, Hinz R, Fuchtner F, Muller M, Steinbach J, Bauer R (2004b) Developmental changes in the activities of aromatic amino acid decarboxylase and catechol-O-methyl transferase in the porcine brain: a positron emission tomography study. Neurosci Lett 364: 159–163

Buchegger F, Bonvin F, Kosinski M, Schaffland AO, Prior J, Reubi JC, Blauenstein P, Tourwe D, Garcia Garayoa E, Bischof Delaloye A (2003) Radiolabeled neurotensin analog, 99mTc-NT-XI, evaluated in ductal pancreatic adenocarcinoma patients. J Nucl Med 44: 1649–1654

Buck A, Nguyen N, Burger C, Ziegler S, Frey L, Weigand G, Erhardt W, Senekowitsch-Schmidtke R, Pellikka R, Blauenstein P, Locher JT, Schwaiger M (1996) Quantitative evaluation of manganese-52 m as a myocardial perfusion tracer in pigs using positron emission tomography. Eur J Nucl Med 23: 1619–1627

Buckman BO, VanBrocklin HF, Dence CS, Bergmann SR, Welch MJ, Katzenellenbogen JA (1994) Synthesis and tissue biodistribution of [omega-^{11}C]palmitic acid. A novel PET imaging agent for cardiac fatty acid metabolism. J Med Chem 37: 2481–2485

Buhler P, Just U, Will E, Kotzerke J, van den Hoff J (2004) An accurate method for correction of head movement in PET. IEEE Trans Med Imaging 23: 1176–1185

Buxton DB, Nienaber CA, Luxen A, Ratib O, Hansen H, Phelps ME, Schelbert HR (1989) Noninvasive quantitation of regional myocardial oxygen consumption *in vivo* with [1-^{11}C]acetate and dynamic positron emission tomography. Circulation 79: 134–142

Chatziioannou A, Tai YC, Doshi N, Cherry SR (2001) Detector development for microPET II: a 1 microl resolution PET scanner for small animal imaging. Phys Med Biol 46: 2899–2910

Chatziioannou AF (2002a) Molecular imaging of small animals with dedicated PET tomographs. Eur J Nucl Med Mol Imaging 29: 98–114

Chatziioannou AF (2002b) PET scanners dedicated to molecular imaging of small animal models. Mol Imaging Biol 4: 47–63

Chen CC, Wang KC (1969) Selenomethionine selenium-75 scintiscanning of the pancreas. Taiwan Yi Xue Hui Za Zhi 68: 341–349

Chen JC, Chang SM, Hsu FY, Wang HE, Liu RS (2004a) MicroPET-based pharmacokinetic analysis of the radiolabeled boron compound [^{18}F]FBPA-F in rats with F98 glioma. Appl Radiat Isot 61: 887–891

Chen X, Park R, Hou Y, Tohme M, Shahinian AH, Bading JR, Conti PS (2004b) MicroPET and autoradiographic imaging of GRP receptor expression with ^{64}Cu-DOTA-[Lys3]bombesin in human prostate adenocarcinoma xenografts. J Nucl Med 45: 1390–1397

Cherry SR (2001) Fundamentals of positron emission tomography and applications in preclinical drug development. J Clin Pharmacol 41: 482–491

Cherry SR, Gambhir SS (2001) Use of positron emission tomography in animal research. ILAR J 42: 219–232

Coenen HH, Kling P, Stocklin G (1989) Cerebral metabolism of L-[2-^{18}F]fluorotyrosine, a new PET tracer of protein synthesis. J Nucl Med 30: 1367–1372

Colby LA, Morenko BJ (2004) Clinical considerations in rodent bioimaging. Comp Med 54: 623–630

Collingridge DR, Carroll VA, Glaser M, Aboagye EO, Osman S, Hutchinson OC, Barthel H, Luthra SK, Brady F, Bicknell R, Price P, Harris AL (2002a) The development of [^{124}I]iodinated-VG76e: a novel tracer for imaging vascular endothelial growth factor *in vivo* using positron emission tomography. Cancer Res 62: 5912–5919

Comar D, Cartron J, Maziere M, Marazano C (1976) Labelling and metabolism of methionine-methyl-11-C. Eur J Nucl Med 1: 11–14

Couturier O, Luxen A, Chatal JF, Vuillez JP, Rigo P, Hustinx R (2004) Fluorinated tracers for imaging cancer with positron emission tomography. Eur J Nucl Med Mol Imaging 31: 1182–1206

Crawford DC, Flower MA, Pratt BE, Hill C, Zweit J, McCready VR, Harmer CL (1997) Thyroid volume measurement in thyrotoxic patients: comparison between ultrasonography and iodine-124 positron emission tomography. Eur J Nucl Med 24: 1470–1478

Croteau E, Benard F, Cadorette J, Gauthier ME, Aliaga A, Bentourkia M, Lecomte R (2003) Quantitative gated PET for the assessment of left ventricular function in small animals. J Nucl Med 44: 1655–1661

Croteau E, Benard F, Bentourkia M, Rousseau J, Paquette M, Lecomte R (2004) Quantitative myocardial perfusion and coronary reserve in rats with 13N-ammonia and small animal PET: impact of anesthesia and pharmacologic stress agents. J Nucl Med 45: 1924–1930

Cumming P, Hausser M, Martin WR, Grierson J, Adam MJ, Ruth TJ, McGeer EG (1988) Kinetics of *in vitro* decarboxylation and the *in vivo* metabolism of 2-^{18}F- and 6-^{18}F-fluorodopa in the hooded rat. Biochem Pharmacol 37: 247–250

d'Argy R, Paul R, Frankenberg L, Stalnacke CG, Lundqvist H, Kangas L, Halldin C, Nagren K, Roeda D, Haaparanta M, et al (1988) Comparative double-tracer whole-body autoradiography: uptake of $^{11}C^{-}$, $^{18}F^{-}$ and 3H-labeled compounds in rat tumors. Int J Rad Appl Instrum B 15: 577–585

Daemen BJ, Zwertbroek R, Elsinga PH, Paans AM, Doorenbos H, Vaalburg W (1991) PET studies with L-[1-^{11}C]tyrosine, L-[methyl-^{11}C]methionine and ^{18}F-fluorodeoxyglucose in prolactinomas in relation to bromocryptine treatment. Eur J Nucl Med 18: 453–460

Daemen BJ, Elsinga PH, Paans AM, Wieringa AR, Konings AW, Vaalburg W (1992) Radiation-induced inhibition of tumor growth as monitored by PET using L-[1-^{11}C]tyrosine and fluorine-18-fluorodeoxyglucose. J Nucl Med 33: 373–379

Daghighian F, Pentlow KS, Larson SM, Graham MC, DiResta GR, Yeh SD, Macapinlac H, Finn RD, Arbit E, Cheung NK (1993) Development of a method to measure kinetics of radiolabelled monoclonal antibody in human tumour with applications to microdosimetry: positron emission tomography studies of iodine-124 labelled 3F8 monoclonal antibody in glioma. Eur J Nucl Med 20: 402–409

Daugherty A, Kilbourn MR, Dence CS, Sobel BE, Thorpe SR (1992) Quantitative assessment of lipoprotein metabolism by positron emission tomography with an ^{18}F-containing residualizing label. Int J Rad Appl Instrum B 19: 411–416

de Graaf C, Blom WA, Smeets PA, Stafleu A, Hendriks HF (2004) Biomarkers of satiation and satiety. Am J Clin Nutr 79: 946–961

de Vries EF, Vroegh J, Dijkstra G, Moshage H, Elsinga PH, Jansen PL, Vaalburg W (2004) Synthesis and evaluation of a fluorine-18 labeled antisense oligonucleotide as a potential PET tracer for iNOS mRNA expression. Nucl Med Biol 31: 605–612

Debruyne D, Sobrio F, Hinschberger A, Camsonne R, Coquerel A, Barre L (2003) Short-term pharmacokinetics and brain distribution of mecamylamine as a preliminary to carbon-11 labeling for nicotinic receptor investigation. J Pharm Sci 92: 1051–1057

Defrise M, Kinahan PE, Townsend DW, Michel C, Sibomana M, Newport DF (1997) Exact and approximate rebinning algorithms for 3-D PET data. IEEE Trans Med Imaging 16: 145–158

DeGrado TR, Coenen HH, Stocklin G (1991) 14(R,S)-[^{18}F]fluoro-6-thia-heptadecanoic acid (FTHA): evaluation in mouse of a new probe of myocardial utilization of long chain fatty acids. J Nucl Med 32: 1888–1896

DeGrado TR, Wang S, Holden JE, Nickles RJ, Taylor M, Stone CK (2000) Synthesis and preliminary evaluation of ^{18}F-labeled 4-thia palmitate as a PET tracer of myocardial fatty acid oxidation. Nucl Med Biol 27: 221–231

DeJesus OT, Holden JE, Endres C, Murali D, Oakes TR, Shelton S, Uno H, Houser D, Freund L, Perlman SB, et al (1992) Visualization of dopamine nerve terminals by positron tomography using [^{18}F]fluoro-beta-fluoromethylene-m-tyrosine. Brain Res 597: 151–154

DeJesus OT, Murali D, Kitchen R, Endres C, Oakes TR, Shelton SE, Freund L, Houser D, Uno H, Holden JE, et al (1994) Evaluation of 3-[^{18}F]fluoro-alpha-fluoromethyl-p-tyrosine as a tracer for striatal tyrosine hydroxylase activity. Nucl Med Biol 21: 663–667

Dekker B, Keen H, Lyons S, Disley L, Hastings D, Reader A, Ottewell P, Watson A, Zweit J (2005) MBP-annexin V radiolabeled directly with iodine-124 can be used to image apoptosis *in vivo* using PET. Nucl Med Biol 32: 241–252

Del Rosario RB, Mangner TJ, Gildersleeve DL, Shreve PD, Weiland DM, Lowe JA 3rd, Drozda SE, Snider RM (1993) Synthesis of a nonpeptide carbon-11 labeled substance P antagonist for PET studies. Nucl Med Biol 20: 545–547

Doudet DJ, McLellan CA, Carson R, Adams HR, Miyake H, Aigner TG, Finn RT, Cohen RM (1991) Distribution and kinetics of 3-O-methyl-6-[^{18}F]fluoro-L-dopa in the rhesus monkey brain. J Cereb Blood Flow Metab 11: 726–734

Duatti A (2004) *In vivo* imaging of oligonucleotides with nuclear tomography. Curr Drug Targets 5: 753–760

Duffy TE, Cavazzuti M, Cruz NF, Sokoloff L (1982) Local cerebral glucose metabolism in newborn dogs: effects of hypoxia and halothane anesthesia. Ann Neurol 11: 233–246

Ellis BL, Sharma HL (1999) Co, Fe and Ga chelates for cell labelling: a potential use in PET imaging? Nucl Med Commun 20: 1017–1021

Eriksson B, Bergstrom M, Lilja A, Ahlstrom H, Langstrom B, Oberg K (1993) Positron emission tomography (PET) in neuroendocrine gastrointestinal tumors. Acta Oncol 32: 189–196

Eschgfaller B, Konig M, Boess F, Boelsterli UA, Benner SA (1998) Synthesis and biodistribution of a short nonionic oligonucleotide analogue in mouse with a potential to mimic peptides. J Med Chem 41: 276–283

Eschmann SM, Reischl G, Bilger K, Kupferschlager J, Thelen MH, Dohmen BM, Besenfelder H, Bares R (2002) Evaluation of dosimetry of radioiodine therapy in benign and malignant thyroid disorders by means of iodine-124 and PET. Eur J Nucl Med Mol Imaging 29: 760–767

Farquhar TH, Chatziioannou A, Cherry SR (1998) An evaluation of exact and approximate 3-D reconstruction algorithms for a high-resolution, small-animal PET scanner. IEEE Trans Med Imaging 17: 1073–1080

Flower MA, al-Saadi A, Harmer CL, McCready VR, Ott RJ (1994) Dose-response study on thyrotoxic patients undergoing positron emission tomography and radioiodine therapy. Eur J Nucl Med 21: 531–536

Foster AC, Fagg GE (1984) Acidic amino acid binding sites in mammalian neuronal membranes: their characteristics and relationship to synaptic receptors. Brain Res 319: 103–164

Fowler JS, Ido T (2002) Initial and subsequent approach for the synthesis of ^{18}FDG. Semin Nucl Med 32: 6–12

Freudenberg LS, Antoch G, Gorges R, Knust J, Pink R, Jentzen W, Debatin JF, Brandau W, Bockisch A, Stattaus J (2003) Combined PET/CT with iodine-124 in diagnosis of spread metastatic thyroid carcinoma: a case report. Eur Radiol 13 [Suppl 4]: L19–L23

Fujibayashi Y, Saji H, Yomoda I, Kawai K, Horiuchi K, Adachi H, Torizuka K, Yokoyama A (1986) ^{62}Zn-EDDA: a radiopharmaceutical for pancreatic functional diagnosis. Int J Nucl Med Biol 12: 439–446

Garcia-Garayoa E, Blauenstein P, Bruehlmeier M, Blanc A, Iterbeke K, Conrath P, Tourwe D, Schubiger PA (2002) Preclinical evaluation of a new, stabilized neurotensin (8–13) pseudopeptide radiolabeled with (99 m)Tc. J Nucl Med 43: 374–383

Gautier JF, Chen K, Salbe AD, Bandy D, Pratley RE, Heiman M, Ravussin E, Reiman EM, Tataranni PA (2000) Differential brain responses to satiation in obese and lean men. Diabetes 49: 838–846

Geary N, Grotschel H, Scharrer E (1982) Blood metabolites and feeding during postinsulin hypophagia. Am J Physiol 243: R304–R311

Geltman EM (1994) Assessment of myocardial fatty acid metabolism with 1-^{11}C-palmitate. J Nucl Cardiol 1: S15–S22

Geltman EM, Roberts R, Sobel BE (1980) Cardiac positron tomography: current status and future directions. Herz 5: 107–119

German DC, Eisch AJ (2004) Mouse models of Alzheimer's disease: insight into treatment. Rev Neurosci 15: 353–369

Gester S, Wüst F, Pawelke B, Bergmann R, Pietzsch J (2005) Synthesis and biodistribution of an ^{18}F-labelled resveratrol derivative for small animal positron emission tomography. Amino Acids 29: 415–428

Ginj M, Chen J, Walter MA, Eltschinger V, Reubi JC, Maecke HR (2005) Preclinical evaluation of new and highly potent analogues of octreotide for predictive imaging and targeted radiotherapy. Clin Cancer Res 11: 1136–1145

Go KG, Prenen GH, Paans AM, Vaalburg W, Kamman RL, Korf J (1990) Positron emission tomography study of ^{11}C-acetoacetate uptake in a freezing lesion in cat brain, as correlated with ^{11}C-tyrosine and ^{18}F-fluorodeoxyglucose uptake, and with proton magnetic resonance imaging. Adv Neurol 52: 525–528

Goethals P, Volkaert A, Vandewielle C, Dierckx R, Lameire N (2000) ^{55}Co-EDTA for renal imaging using positron emission tomography (PET): a feasibility study. Nucl Med Biol 27: 77–81

Green MV, Seidel J, Vaquero JJ, Jagoda E, Lee I, Eckelman WC (2001) High resolution PET, SPECT and projection imaging in small animals. Comput Med Imaging Graph 25: 79–86

Grierson JR, Yagle KJ, Eary JF, Tait JF, Gibson DF, Lewellen B, Link JM, Krohn KA (2004) Production of [F-18]fluoroannexin for imaging apoptosis with PET. Bioconjug Chem 15: 373–379

Griffiths GL, Chang CH, McBride WJ, Rossi EA, Sheerin A, Tejada GR, Karacay H, Sharkey RM, Horak ID, Hansen HJ, Goldenberg DM (2004) Reagents and methods for PET using bispecific antibody pretargeting and ^{68}Ga-radiolabeled bivalent hapten-peptide-chelate conjugates. J Nucl Med 45: 30–39

Groot-Wassink T, Aboagye EO, Wang Y, Lemoine NR, Reader AJ, Vassaux G (2004) Quantitative imaging of Na/I symporter transgene expression using positron emission tomography in the living animal. Mol Ther 9: 436–442

Guhlke S, Wester HJ, Bruns C, Stocklin G (1994) (2-[^{18}F]fluoropropionyl-(D)phe1)-octreotide, a potential radiopharmaceutical for quantitative somatostatin receptor imaging with PET: synthesis, radiolabeling, *in vitro* validation and biodistribution in mice. Nucl Med Biol 21: 819–825

Haaparanta M, Gronroos T, Marjamaki P, Eskola O, Bergman J, Paul R, Solin O (2004) *In vivo* sampling for pharmacokinetic studies in small experimental animals: a combination of microdialysis, planar chromatography and digital autoradiography. Mol Imaging Biol 6: 27–33

Halldin C, Schoeps KO, Stone-Elander S, Wiesel FA (1987) The Bucherer-Strecker synthesis of D- and L-(1-^{11}C)tyrosine and the *in vivo* study of L-(1-^{11}C)tyrosine in human brain using positron emission tomography. Eur J Nucl Med 13: 288–291

Hargreaves R (2002) Imaging substance P receptors (NK1) in the living human brain using positron emission tomography. J Clin Psychiatry 63 [Suppl 11]: 18–24

Hawkins RA, Huang SC, Barrio JR, Keen RE, Feng D, Mazziotta JC, Phelps ME (1989) Estimation of local cerebral protein synthesis rates with L-[1-^{11}C]leucine and PET: methods, model, and results in animals and humans. J Cereb Blood Flow Metab 9: 446–460

Hawkins RA, Choi Y, Huang SC, Hoh CK, Dahlbom M, Schiepers C, Satyamurthy N, Barrio JR, Phelps ME (1992) Evaluation of the skeletal kinetics of fluorine-18-fluoride ion with PET. J Nucl Med 33: 633–642

Hayase N, Tomiyoshi K, Watanabe K, Horikoshi S, Shibasaki T, Ohye C (1995) Positron emission tomography with 4-[^{18}F]fluoro-L-m-tyrosine in MPTP-induced hemiparkinsonian monkeys. Ann Nucl Med 9: 119–123

Heinrichs U, Bruyndonckx P, Choi Y, Dietzel G, Korjik M, Lecoq P, Morel C, Pedrini C, Petrosyan AG, Pietrzyk U, Sappey-Marinier D, Streun M, Tavernier S, Ziemons K (2004) The ClearPET (TM): a high resolution high sensitivity dual-layer phoswich small animal PET scanner. Eur J Nucl Med Mol Imaging 31: S400

Henriksen G, Schottelius M, Poethko T, Hauser A, Wolf I, Schwaiger M, Wester HJ (2004) Proof of principle for the use of ^{11}C-labelled peptides

in tumour diagnosis with PET. Eur J Nucl Med Mol Imaging 31: 1653–1657

Herschman HR (2003) Micro-PET imaging and small animal models of disease. Curr Opin Immunol 15: 378–384

Higashi K, Ueda Y, Matsunari I, Kodama Y, Ikeda R, Miura K, Taki S, Higuchi T, Tonami H, Yamamoto I (2004) ^{11}C-acetate PET imaging of lung cancer: comparison with ^{18}F-FDG PET and 99mTc-MIBI SPET. Eur J Nucl Med Mol Imaging 31: 13–21

Hoegerle S, Juengling F, Otte A, Altehoefer C, Moser EA, Nitzsche EU (1998) Combined FDG and [F-18]fluoride whole-body PET: a feasible two-in-one approach to cancer imaging? Radiology 209: 253–258

Huang SC, Wu HM, Shoghi-Jadid K, Stout DB, Chatziioannou A, Schelbert HR, Barrio JR (2004) Investigation of a new input function validation approach for dynamic mouse microPET studies. Mol Imaging Biol 6: 34–46

Hubner KF, Andrews GA, Buonocore E, Hayes RL, Washburn LC, Collmann IR, Gibbs WD (1979) Carbon-11-labeled amino acids for the rectilinear and positron tomographic imaging of the human pancreas. J Nucl Med 20: 507–513

Hubner KF, Krauss S, Washburn LC, Gibbs WD, Holloway EC (1981) Tumor detection with 1-aminocyclopentane and 1-aminocyclobutane C-11-carboxylic acid using positron emission computerized tomography. Clin Nucl Med 6: 249–252

Iida H, Rhodes CG, de Silva R, Araujo LI, Bloomfield PM, Lammertsma AA, Jones T (1992) Use of the left ventricular time-activity curve as a noninvasive input function in dynamic oxygen-15-water positron emission tomography. J Nucl Med 33: 1669–1677

Ikemoto M, Sasaki M, Haradahira T, Yada T, Omura H, Furuya Y, Watanabe Y, Suzuki K (1999) Synthesis of L-[beta-C-11]amino acids using immobilized enzymes. Appl Radiat Isot 50: 715–721

Ishiwata K, Ido T, Kawamura M, Kubota K, Ichihashi M, Mishima Y (1991) 4-Borono-2-[F-18]fluoro-D,L-phenylalanine as a target compound for boron neutron-capture therapy – tumor imaging potential with positron emission tomography. Int J Radiat Appl Instrum B 18: 745–751

Ishiwata K, Shinoda M, Ishii S, Nozaki T, Senda M (1996) Synthesis and evaluation of an ^{18}F-labeled dopa prodrug as a PET tracer for studying brain dopamine metabolism. Nucl Med Biol 23: 295–301

Ishiwata K, Tsukada H, Kubota K, Nariai T, Harada N, Kawamura K, Kimura Y, Oda K, Iwata R, Ishii K (2005) Preclinical and clinical evaluation of O-[C-11]methyl-L-tyrosine for tumor imaging by positron emission tomography. Nucl Med Biol 32: 253–262

Iwata R, Furumoto S, Pascali C, Bogni A, Ishiwata K (2003) Radiosynthesis of O-[C-11]methyl-L-tyrosine and O-[F-18]fluoromethyl-L-tyrosine as potential PET tracers for imaging amino acid transport. J Labelled Comp Radiopharm 46: 555–566

Iyer M, Barrio JR, Namavari M, Bauer E, Satyamurthy N, Nguyen K, Toyokuni T, Phelps ME, Herschman HR, Gambhir SS (2001) 8-[^{18}F]Fluoropenciclovir: an improved reporter probe for imaging HSV1-tk reporter gene expression *in vivo* using PET. J Nucl Med 42: 96–105

Jager PL, Vaalburg W, Pruim J, de Vries EG, Langen KJ, Piers DA (2001) Radiolabeled amino acids: basic aspects and clinical applications in oncology. J Nucl Med 42: 432–445

Jagoda EM, Aloj L, Seidel J, Lang L, Moody TW, Green S, Caraco C, Daube-Witherspoon M, Green MV, Eckelman WC (2002) Comparison of an ^{18}F labeled derivative of vasoactive intestinal peptide and 2-deoxy-2-[^{18}F]fluoro-D-glucose in nude mice bearing breast cancer xenografts. Mol Imaging Biol 4: 369–379

Jagoda EM, Vaquero JJ, Seidel J, Green MV, Eckelman WC (2004) Experiment assessment of mass effects in the rat: implications for small animal PET imaging. Nucl Med Biol 31: 771–779

Jalilian AR, Rowshanfarzad P, Afarideh H, Shafiee A, Sabet M, Kyoumarsi M, Raisali GR (2004) Synthesis of [^{75}Se]5-ethoxycarbonyl-4-methyl-1,2,3-selenadiazole. Appl Radiat Isot 60: 659–663

Jian R, Vigneron N, Najean Y, Bernier JJ (1982) Gastric emptying and intragastric distribution of lipids in man. A new scintigraphic method of study. Dig Dis Sci 27: 705–711

Johannsen B (2005) The usefulness of radiotracers to make the body biochemically transparent. Amino Acids 29: 307–311

Johnstrom P, Harris NG, Fryer TD, Barret O, Clark JC, Pickard JD, Davenport AP (2002) ^{18}F-Endothelin-1, a positron emission tomography (PET) radioligand for the endothelin receptor system: radiosynthesis and *in vivo* imaging using microPET. Clin Sci 103 [Suppl 48]: 4S–8S

Jones SC, Ackerman RH, Hoop B Jr, Baron JC, Brownell GL, Taveras JM (1983) Brain uptake and organ distribution of ^{11}C from ^{11}C-labeled glucose. Int J Nucl Med Biol 10: 173–180

Kates AM, Herrero P, Dence C, Soto P, Srinivasan M, Delano DG, Ehsani A, Gropler RJ (2003) Impact of aging on substrate metabolism by the human heart. J Am Coll Cardiol 41: 293–299

Keen HG, Dekker BA, Disley L, Hastings D, Lyons S, Reader AJ, Ottewell P, Watson A, Zweit J (2005a) Imaging apoptosis *in vivo* using ^{124}I-annexin V and PET. Nucl Med Biol 32: 395–402

Keiding S, Munk OL, Roelsgaard K, Bender D, Bass L (2001) Positron emission tomography of hepatic first-pass metabolism of ammonia in pig. Eur J Nucl Med 28: 1770–1775

Kenanova V, Olafsen T, Crow DM, Sundaresan G, Subbarayan M, Carter NH, Ikle DN, Yazaki PJ, Chatziioannou AF, Gambhir SS, Williams LE, Shively JE, Colcher D, Raubitschek AA, Wu AM (2005) Tailoring the pharmacokinetics and positron emission tomography imaging properties of anti-carcinoembryonic antigen single-chain Fv-Fc antibody fragments. Cancer Res 65: 622–631

Klein HA, DiSibio KJ, Sims D, Singleton HC, Worthy LJ (2005) I-123 whole body scanning: case report and discussion. Clin Nucl Med 30: 312–316

Knoess C, Siegel S, Smith A, Newport D, Richerzhagen N, Winkeler A, Jacobs A, Goble RN, Graf R, Wienhard K, Heiss WD (2003) Performance evaluation of the microPET R4 PET scanner for rodents. Eur J Nucl Med Mol Imaging 30: 737–747

Kobori N, Imahori Y, Mineura K, Ueda S, Fujii R (1999) Visualization of mRNA expression in CNS using C-11-labeled phosphorothioate oligodeoxynucleotide. Neuroreport 10: 2971–2974

Kornblum HI, Araujo DM, Annala AJ, Tatsukawa KJ, Phelps ME, Cherry SR (2000) *In vivo* imaging of neuronal activation and plasticity in the rat brain by high resolution positron emission tomography (microPET). Nat Biotechnol 18: 655–660

Krivokapich J, Keen RE, Phelps ME, Shine KI, Barrio JR (1987) Effects of anoxia on kinetics of [^{13}N] glutamate and $^{13}NH_3$ metabolism in rabbit myocardium. Circ Res 60: 505–516

Kubota K, Fukuda H, Yamada K, Endo S, Ito M, Abe Y, Yamaguchi T, Fujiwara T, Sato T, Yamaura H, et al (1983) Experimental pancreas imaging study with ^{13}N-glutamate using positron computer tomography. Eur J Nucl Med 8: 528–530

Kubota K, Ishiwata K, Kubota R, Yamada S, Takahashi J, Abe Y, Fukuda H, Ido T (1996) Feasibility of fluorine-18-fluorophenylalanine for tumor imaging compared with carbon-11-L-methionine. J Nucl Med 37: 320–325

Kuhnast B, Hinnen F, Hamzavi R, Boisgard R, Tavitian B, Nielsen PE, Dolle F (2005) Fluorine-18 labelling of PNAs functionalized at their pseudo-peptidic backbone for imaging studies with PET. J Labelled Comp Radiopharm 48: 51–61

Lammertsma AA, Hume SP (1996) Simplified reference tissue model for PET receptor studies. Neuroimage 4: 153–158

Lange CW, VanBrocklin HF, Taylor SE (2002) Photoconjugation of 3-azido-5-nitrobenzyl-[F-18]fluoride to an oligonucleotide aptamer. J Labelled Comp Radiopharm 45: 257–268

Langen KJ, Borner AR, Muller-Mattheis V, Hamacher K, Herzog H, Ackermann R, Coenen HH (2001) Uptake of cis-4-[^{18}F]fluoro-L-proline in urologic tumors. J Nucl Med 42: 752–754

Larson SM, Pentlow KS, Volkow ND, Wolf AP, Finn RD, Lambrecht RM, Graham MC, Di Resta G, Bendriem B, Daghighian F, et al (1992) PET scanning of iodine-124-3F9 as an approach to tumor dosimetry during treatment planning for radioimmunotherapy in a child with neuroblastoma. J Nucl Med 33: 2020–2023

Laverman P, Boerman OC, Corstens FH, Oyen WJ (2002) Fluorinated amino acids for tumour imaging with positron emission tomography. Eur J Nucl Med Mol Imaging 29: 681–690

Lecomte R (2004) Technology challenges in small animal PET imaging. Nuclear Instruments & Methods in Physics Research Section A – Accelerators Spectrometers Detectors and Associated Equipment 527: 157–165

Lecomte R, Croteau E, Gauthier ME, Archambault M, Aliaga A, Rousseau J, Cadorette J, Leroux JD, Lepage MD, Benard F, Bentourkia M (2004) Cardiac PET imaging of blood flow, metabolism, and function in normal and infarcted rats. IEEE Trans Nucl Sci 51: 696–704

Leenders KL, Poewe WH, Palmer AJ, Brenton DP, Frackowiak RS (1986) Inhibition of L-[^{18}F]fluorodopa uptake into human brain by amino acids demonstrated by positron emission tomography. Ann Neurol 20: 258–262

Lendvai G, Velikyan I, Bergstrom M, Estrada S, Laryea D, Valila M, Salomaki S, Langstrom B, Roivainen A (2005) Biodistribution of ^{68}Ga-labelled phosphodiester, phosphorothioate, and 2′-O-methyl phosphodiester oligonucleotides in normal rats. Eur J Pharm Sci 26(1): 26–38

Levchenko A, Mehta BM, Lee JB, Humm JL, Augensen F, Squire O, Kothari PJ, Finn RD, Leonard EF, Larson SM (2000) Evaluation of ^{11}C-colchicine for PET imaging of multiple drug resistance. J Nucl Med 41: 493–501

Lewis JS, Lewis MR, Srinivasan A, Schmidt MA, Wang J, Anderson CJ (1999) Comparison of four ^{64}Cu-labeled somatostatin analogues *in vitro* and in a tumor-bearing rat model: evaluation of new derivatives for positron emission tomography imaging and targeted radiotherapy. J Med Chem 42: 1341–1347

Lewis MR, Reichert DE, Laforest R, Margenau WH, Shefer RE, Klinkowstein RE, Hughey BJ, Welch MJ (2002) Production and purification of gallium-66 for preparation of tumor-targeting radiopharmaceuticals. Nucl Med Biol 29: 701–706

Lewis MR, Wang M, Axworthy DB, Theodore LJ, Mallet RW, Fritzberg AR, Welch MJ, Anderson CJ (2003) *In vivo* evaluation of pretargeted ^{64}Cu for tumor imaging and therapy. J Nucl Med 44: 1284–1292

Li SR, Beheshti M (2005) The radionuclide molecular imaging and therapy of neuroendocrine tumors. Curr Cancer Drug Targets 5: 139–148

Liu RS, Chang CP, Chu YK, Chu LS, Chang CW, Wu LC, Yeh SH (2001) C-11-acetate is a metabolic substrate for synthesis of amino acid in glioma: *in-vivo* evidence on PET. J Nucl Med 42: 231P–231P

Liu X, Comtat C, Michel C, Kinahan P, Defrise M, Townsend D (2001) Comparison of 3-D reconstruction with 3D-OSEM and with FORE + OSEM for PET. IEEE Trans Med Imaging 20: 804–814

Lovqvist A, Sundin A, Ahlstrom H, Carlsson J, Lundqvist H (1997) Pharmacokinetics and experimental PET imaging of a bromine-76-labeled monoclonal anti-CEA antibody. J Nucl Med 38: 395–401

Lyons SK (2005) Advances in imaging mouse tumour models *in vivo*. J Pathol 205: 194–205

Lundqvist H, Tolmachev V (2002) Targeting peptides and positron emission tomography. Biopolymers 66: 381–392

Maecke HR, Hofmann M, Haberkorn U (2005) ^{68}Ga-labeled peptides in tumor imaging. J Nucl Med 46 [Suppl 1]: 172S–178S

Maina T, Nock BA, Zhang H, Nikolopoulou A, Waser B, Reubi JC, Maecke HR (2005) Species differences of bombesin analog interactions with GRP-R define the choice of animal models in the development of GRP-R-targeting drugs. J Nucl Med 46: 823–830

Martarello L, McConathy J, Camp VM, Malveaux EJ, Simpson NE, Simpson CP, Olson JJ, Bowers GD, Goodman MM (2002) Synthesis of syn- and anti-1-amino-3-[^{18}F]fluoromethyl-cyclobutane-1-carboxylic acid (FMACBC), potential PET ligands for tumor detection. J Med Chem 45: 2250–2259

Mathias CJ, Lewis MR, Reichert DE, Laforest R, Sharp TL, Lewis JS, Yang ZF, Waters DJ, Snyder PW, Low PS, Welch MJ, Green MA (2003) Preparation of Ga-66- and Ga-68-labeled Ga(III)-deferoxamine-folate as potential folate-receptor-targeted PET radiopharmaceuticals. Nucl Med Biol 30: 725–731

Matsumura A, Mizokawa S, Tanaka M, Wada Y, Nozaki S, Nakamura F, Shiomi S, Ochi H, Watanabe Y (2003) Assessment of microPET performance in analyzing the rat brain under different types of anesthesia: comparison between quantitative data obtained with microPET and ex vivo autoradiography. Neuroimage 20: 2040–2050

Maziere B, Stulzaft O, Verret JM, Comar D, Syrota A (1983) [^{55}Co]- and [^{64}Cu]DTPA: new radiopharmaceuticals for quantitative tomocisternography. Int J Appl Radiat Isot 34: 595–601

McCarthy TJ, Banks WA, Farrell CL, Adamu S, Derdeyn CP, Snyder AZ, Laforest R, Litzinger DC, Martin D, LeBel CP, Welch MJ (2002) Positron emission tomography shows that intrathecal leptin reaches the hypothalamus in baboons. J Pharmacol Exp Ther 301: 878–883

McConathy J, Martarello L, Malveaux EJ, Camp VM, Simpson NE, Simpson CP, Bowers GD, Olson JJ, Goodman MM (2002) Radiolabeled amino acids for tumor imaging with PET: radiosynthesis and biological evaluation of 2-amino-3-[^{18}F]fluoro-2-methylpropanoic acid and 3-[^{18}F]fluoro-2-methyl-2-(methylamino)propanoic acid. J Med Chem 45: 2240–2249

McConnell KP (1959) Selenium-75-binding in dog leucocytes. Tex Rep Biol Med 17: 120–122

McConnell KP, Roth DM (1968) Incorporation of selenium-75-labeled rat plasma proteins into rat liver ribosomes. Arch Biochem Biophys 125: 29–34

McElroy DP, Pimpl W, Pichler BJ, Rafecas M, Schuler T, Ziegler SI (2005) Characterization and readout of MADPET-II detector modules: validation of a unique design concept for high resolution small animal PET. IEEE Trans Nucl Sci 52: 199–204

Melega WP, Perlmutter MM, Luxen A, Nissenson CH, Grafton ST, Huang SC, Phelps ME, Barrio JR (1989) 4-[^{18}F]fluoro-L-m-tyrosine: an L-3,4-dihydroxyphenylalanine analog for probing presynaptic dopaminergic function with positron emission tomography. J Neurochem 53: 311–314

Meyer GJ, Macke H, Schuhmacher J, Knapp WH, Hofmann M (2004) ^{68}Ga-labelled DOTA-derivatised peptide ligands. Eur J Nucl Med Mol Imaging 31: 1097–1104

Middleton E Jr, Kandaswami C, Theoharides TC (2000) The effects of plant flavonoids on mammalian cells: implications for inflammation, heart disease, and cancer. Pharmacol Rev 52: 673–751

Mitterhauser M, Wadsak W, Wabnegger L, Sieghart W, Viernstein H, Kletter K, Dudczak R (2003) *In vivo* and *in vitro* evaluation of [^{18}F]FETO with respect to the adrenocortical and GABAergic system in rats. Eur J Nucl Med Mol Imaging 30: 1398–1401

Moerlein SM, Daugherty A, Sobel BE, Welch MJ (1991) Metabolic imaging with gallium-68- and indium-111-labeled low-density lipoprotein. J Nucl Med 32: 300–307

Momosaki S, Hatano K, Kawasumi Y, Kato T, Hosoi R, Kobayashi K, Inoue O, Ito K (2004) Rat-PET study without anesthesia: anesthetics modify the dopamine D-1 receptor binding in rat brain. Synapse 54: 207–213

Moon BS, Kim SW, Lee TS, Ahn SH, Lee KC, An GI, Yang SD, Chi DY, Choi CW, Lim SM, Chun KS (2005) Synthesis of O-(3-[F-18]fluoropropyl)-L-tyrosine (L-[F-18]FPT) and its biological evaluation in 9L tumor bearing rat. Bull Korean Chem Soc 26: 91–96

Moore TH, Osteen TL, Chatziioannou TF, Hovda DA, Cherry TR (2000) Quantitative assessment of longitudinal metabolic changes *in vivo* after traumatic brain injury in the adult rat using FDG-microPET. J Cereb Blood Flow Metab 20: 1492–1501

Murakami Y, Takamatsu H, Taki J, Tatsumi M, Noda A, Ichise R, Tait JF, Nishimura S (2004) ^{18}F-labelled annexin V: a PET tracer for apoptosis imaging. Eur J Nucl Med Mol Imaging 31: 469–474

Myers R (2001) The biological application of small animal PET imaging. Nucl Med Biol 28: 585–593

Nabulsi NB, Smith DE, Kilbourn MR (2005) [^{11}C]Glycylsarcosine: synthesis and *in vivo* evaluation as a PET tracer of PepT2 transporter function in kidney of PepT2 null and wild-type mice. Bioorg Med Chem 13: 2993–3001

Nader MA, Grant KA, Gage HD, Ehrenkaufer RL, Kaplan JR, Mach RH (1999) PET imaging of dopamine D2 receptors with [^{18}F]fluoroclebopride in monkeys: effects of isoflurane- and ketamine-induced anesthesia. Neuropsychopharmacology 21: 589–596

Nahapetian AT, Janghorbani M, Young VR (1983) Urinary trimethylselenonium excretion by the rat: effect of level and source of selenium-75. J Nutr 113: 401–411

Ng CK, Huang SC, Schelbert HR, Buxton DB (1994) Validation of a model for [1-^{11}C]acetate as a tracer of cardiac oxidative metabolism. Am J Physiol 266: H1304–H1315

Noda A, Ohba H, Kakiuchi T, Futatsubashi M, Tsukada H, Nishimura S (2002) Age-related changes in cerebral blood flow and glucose metabolism in conscious rhesus monkeys. Brain Res 936: 76–81

Noda A, Takamatsu H, Minoshima S, Tsukada H, Nishimura S (2003) Determination of kinetic rate constants for 2-[^{18}F]fluoro-2-deoxy-D-glucose and partition coefficient of water in conscious macaques and alterations in aging or anesthesia examined on parametric images with an anatomic standardization technique. J Cereb Blood Flow Metab 23: 1441–1447

Oberdorfer F, Zobeley A, Weber K, Prenant C, Haberkorn U, Maierborst W (1993) Preparation of alpha-[3-C-11]aminoisobutyric acid from an azadisilolidine derivative of alanine. J Labelled Compd Radiopharm 33: 345–353

Okazawa H, Fujibayashi Y, Yonekura Y, Tamaki N, Nishizawa S, Magata Y, Ishizu K, Tsuchida T, Sadato N, Konishi J, et al (1995) Clinical application of ^{62}Zn/^{62}Cu positron generator: perfusion and plasma pool images in normal subjects. Ann Nucl Med 9: 81–87

Olafsen T, Cheung CW, Yazaki PJ, Li L, Sundaresan G, Gambhir SS, Sherman MA, Williams LE, Shively JE, Raubitschek AA, Wu AM (2004) Covalent disulfide-linked anti-CEA diabody allows site-specific conjugation and radiolabeling for tumor targeting applications. Protein Eng Des Sel 17: 21–27

Otsuka FL, Welch MJ, Kilbourn MR, Dence CS, Dilley WG, Wells SA Jr (1991) Antibody fragments labeled with fluorine-18 and gallium-68: *in vivo* comparison with indium-111 and iodine-125-labeled fragments. Int J Radiat Appl Instrum B 18: 813–816

Oyama N, Kim J, Jones LA, Mercer NM, Engelbach JA, Sharp TL, Welch MJ (2002) MicroPET assessment of androgenic control of glucose and acetate uptake in the rat prostate and a prostate cancer tumor model. Nucl Med Biol 29: 783–790

Oyama N, Miller TR, Dehdashti F, Siegel BA, Fischer KC, Michalski JM, Kibel AS, Andriole GL, Picus J, Welch MJ (2003) ^{11}C-acetate PET imaging of prostate cancer: detection of recurrent disease at PSA relapse. J Nucl Med 44: 549–555

Paans AM, Vaalburg W (2000) Positron emission tomography in drug development and drug evaluation. Curr Pharm Des 6: 1583–1591

Pain F, Laniece P, Mastrippolito R, Gervais P, Hantraye P, Besret L (2004) Arterial input function measurement without blood sampling using a beta-microprobe in rats. J Nucl Med 45: 1577–1582

Pan D, Gambhir SS, Toyokuni T, Iyer MR, Acharya N, Phelps ME, Barrio JR (1998) Rapid synthesis of a 5′-fluorinated oligodeoxynucleotide: a model antisense probe for use in imaging with positron emission tomography (PET). Bioorg Med Chem Lett 8: 1317–1320

Pauwels S, Barone R, Walrand S, Borson-Chazot F, Valkema R, Kvols LK, Krenning EP, Jamar F (2005) Practical dosimetry of peptide receptor radionuclide therapy with Y-90-labeled somatostatin analogs. J Nucl Med 46: 92S–98S

Pawelke B (2005) Metabolite analysis in positron emission tomography studies: examples from food sciences. Amino Acids 29: 377–388

Pentlow KS, Graham MC, Lambrecht RM, Cheung NK, Larson SM (1991) Quantitative imaging of I-124 using positron emission tomography with applications to radioimmunodiagnosis and radioimmunotherapy. Med Phys 18: 357–366

Pentlow KS, Graham MC, Lambrecht RM, Daghighian F, Bacharach SL, Bendriem B, Finn RD, Jordan K, Kalaigian H, Karp JS, Robeson WR, Larson SM (1996) Quantitative imaging of iodine-124 with PET. J Nucl Med 37: 1557–1562

Pestourie C, Tavitian B, Duconge F (2005) Aptamers against extracellular targets for *in vivo* applications. Biochimie 87(9–10): 921–930

Phelps ME, Huang SC, Hoffman EJ, Selin C, Sokoloff L, Kuhl DE (1979) Tomographic measurement of local cerebral glucose metabolic rate in humans with (F-18)2-fluoro-2-deoxy-D-glucose: validation of method. Ann Neurol 6: 371–388

Piert M, Zittel TT, Becker GA, Jahn M, Stahlschmidt A, Maier G, Machulla HJ, Bares R (2001) Assessment of porcine bone metabolism by dynamic [F-18]fluoride ion PET: correlation with bone histomorphometry. J Nucl Med 42: 1091–1100

Piert M, Zittel TT, Jahn M, Stahlschmidt A, Becker GA, Machulla HJ (2003) Increased sensitivity in detection of a porcine high-turnover osteopenia after total gastrectomy by dynamic ^{18}F-fluoride ion PET and quantitative CT. J Nucl Med 44: 117–124

Pietzsch J, Bergmann R, Wuest F, Pawelke B, van den Hoff J (2004) Assessment of metabolism of native and oxidized low density lipoprotein *in vivo*: insights from animal positron emission tomography (microPET) studies. Atherosclerosis [Suppl 5]: 143–144

Pietzsch J, Bergmann R, Wuest F, van den Hoff J (2005a) *In vivo* metabolism of oxidized low density lipoproteins: insights from small animal positron emission tomography (PET) studies. Rec Res Dev Mol Cell Biochem (in press)

Pietzsch J, Bergmann R, Wuest F, Pawelke B, Hultsch C, van den Hoff J (2005b) Catabolism of native and oxidized low density lipoproteins: *in vivo* insights from small animal positron emission tomography studies. Amino Acids 29: 389–404

Plenevaux A, Guillaume M, Brihaye C, Lemaire C, Cantineau R (1990) Chemical processing for production of no-carrier-added selenium-73 from germanium and arsenic targets and synthesis of L-2-amino-4-([^{73}Se]methylseleno) butyric acid (L-[^{73}Se]selenomethionine). Int J Radiat Appl Instrum [A] 41: 829–838

Poetzsch C, Beuthien-Baumann B, van den Hoff J (2003) Teilautomatisierte Segmentierung zur Quantifizierung von Metastasen bei der FDG-PET. Nuklearmedizin 42: 26

Prenant C, Theobald A, Siegel T, Joachim J, Weber K, Haberkorn U, Oberdorfer F (1995) C-11 labeled analogs of alanine by the strecker synthesis. J Labelled Compd Radiopharm 36: 579–586

Prenen GH, Go KG, Paans AM, Zuiderveen F, Vaalburg W, Kamman RL, Molenaar WM, Zijlstra S, Elsinga PH, Sebens JB, et al (1989) Positron emission tomographical studies of 1-^{11}C-acetoacetate, 2-^{18}F-fluorodeoxy-D-glucose, and L-1-^{11}C-tyrosine uptake by cat brain with an experimental lesion. Acta Neurochir (Wien) 99: 166–172

Rapoport SI (2001) *In vivo* fatty acid incorporation into brain phospholipids in relation to plasma availability, signal transduction and membrane remodeling. J Mol Neurosci 16: 243–261

Rasmussen I, Sorensen J, Langstrom B, Haglund U (2004) Is positron emission tomography using ^{18}F-fluorodeoxyglucose and ^{11}C-acetate valuable in diagnosing indeterminate pancreatic masses? Scand J Surg 93: 191–197

Reiffers S, Beerling-van der Molen HD, Vaalburg W, Ten Hoeve W, Paans AM, Korf J, Woldring MG, Wynberg H (1977) Rapid synthesis and purification of carbon-11 labelled DOPA: a potential agent for brain studies. Int J Appl Radiat Isot 28: 955–958

Reubi JC (2003) Peptide receptors as molecular targets for cancer diagnosis and therapy. Endocr Rev 24: 389–427

Reubi JC, Macke HR, Krenning EP (2005) Candidates for peptide receptor radiotherapy today and in the future. J Nucl Med 46 [Suppl 1]: 67S–75S

Riccabona G, Decristoforo C (2003) Peptide targeted imaging of cancer. Cancer Biother Radiopharm 18: 675–687

Robbins RJ (1996) Somatostatin and cancer. Metabolism 45: 98–100

Robinson MK, Doss M, Shaller C, Narayanan D, Marks JD, Adler LP, Gonzalez Trotter DE, Adams GP (2005) Quantitative immuno-positron emission tomography imaging of HER2-positive tumor xenografts with an iodine-124 labeled anti-HER2 diabody. Cancer Res 65: 1471–1478

Rogers BE, Bigott HM, McCarthy DW, Della Manna D, Kim J, Sharp TL, Welch MJ (2003) MicroPET imaging of a gastrin-releasing peptide receptor-positive tumor in a mouse model of human prostate cancer using a ^{64}Cu-labeled bombesin analogue. Bioconjug Chem 14: 756–763

Roivainen A, Tolvanen T, Salomaki S, Lendvai G, Velikyan I, Numminen P, Valila M, Sipila H, Bergstrom M, Harkonen P, Lonnberg H, Langstrom B (2004) ^{68}Ga-labeled oligonucleotides for *in vivo* imaging with PET. J Nucl Med 45: 347–355

Roselt P, Meikle S, Kassiou M (2004) The role of positron emission tomography in the discovery and development of new drugs; as studied in laboratory animals. Eur J Drug Metab Pharmacokinet 29: 1–6

Rowland DJ, Lewis JS, Welch MJ (2002) Molecular imaging: the application of small animal positron emission tomography. J Cell Biochem [Suppl 39]: 110–115

Rubins DJ, Melega WP, Lacan G, Way B, Plenevaux A, Luxen A, Cherry SR (2003) Development and evaluation of an automated atlas-based image analysis method for microPET studies of the rat brain. Neuroimage 20: 2100–2118

Schafers KP (2003) Imaging small animals with positron emission tomography. Nuklearmedizin 42: 86–89

Schelbert HR (2000) PET contributions to understanding normal and abnormal cardiac perfusion and metabolism. Ann Biomed Eng 28: 922–929

Schmidt KC, Cook MP, Qin M, Kang J, Burlin TV, Smith CB (2005) Measurement of regional rates of cerebral protein synthesis with L-[1-^{11}C]leucine and PET with correction for recycling of tissue amino acids: I. Kinetic modeling approach. J Cereb Blood Flow Metab 25: 617–628

Schoder H, Larson SM (2004) Positron emission tomography for prostate, bladder, and renal cancer. Semin Nucl Med 34: 274–292

Schottelius M, Poethko T, Herz M, Reubi JC, Kessler H, Schwaiger M, Wester HJ (2004) First F-18-labeled tracer suitable for routine clinical imaging of sst receptor-expressing tumors using positron emission tomography. Clin Cancer Res 10: 3593–3606

Schuhmacher J, Zhang H, Doll J, Macke HR, Matys R, Hauser H, Henze M, Haberkorn U, Eisenhut M (2005) GRP receptor-targeted PET of a rat pancreas carcinoma xenograft in nude mice with a ^{68}Ga-labeled bombesin (6–14) analog. J Nucl Med 46: 691–699

Schultze B, Oehlert W, Maurer W (1960) [Comparative autoradiographic studies with H-3-, and S-35-labelled amino acids on the protein metabolism of various tissues and cell types in the mouse, rat and rabbit.]. Beitr Pathol Anat 122: 406–431

Seidel J, Vaquero JJ, Green MV (2003) Resolution uniformity and sensitivity of the NIH ATLAS small animal PET scanner: comparison to simulated LSO scanners without depth-of-interaction capability. IEEE Trans Nucl Sci 50: 1347–1350

Seitz U, Wagner M, Vogg AT, Glatting G, Neumaier B, Greten FR, Schmid RM, Reske SN (2001) *In vivo* evaluation of 5-[^{18}F]fluoro-2′-deoxyuridine as tracer for positron emission tomography in a murine pancreatic cancer model. Cancer Res 61: 3853–3857

Setyawati IA, Thompson KH, Yuen VG, Sun Y, Battell M, Lyster DM, Vo C, Ruth TJ, Zeisler S, McNeill JH, Orvig C (1998) Kinetic analysis and comparison of uptake, distribution, and excretion of ^{48}V-labeled compounds in rats. J Appl Physiol 84: 569–575

Sharma H, Zweit J, Smith AM, Downey S (1986) Production of cobalt-55, a short-lived, positron emitting radiolabel for bleomycin. Int J Rad Appl Instrum [A] 37: 105–109

Shaul M, Abourbeh G, Jacobson O, Rozen Y, Laky D, Levitzki A, Mishani E (2004) Novel iodine-124 labeled EGFR inhibitors as potential PET agents for molecular imaging in cancer. Bioorg Med Chem 12: 3421–3429

Shimoji K, Ravasi L, Schmidt K, Soto-Montenegro ML, Esaki T, Seidel J, Jagoda E, Sokoloff L, Green MV, Eckelman WC (2004) Measurement of cerebral glucose metabolic rates in the anesthetized rat by dynamic scanning with ^{18}F-FDG, the ATLAS small animal PET scanner, and arterial blood sampling. J Nucl Med 45: 665–672

Shoup TM, Fischman AJ, Jaywook S, Babich JW, Strauss HW, Elmaleh DR (1994) Synthesis of fluorine-18-labeled biotin derivatives: biodistribution and infection localization. J Nucl Med 35: 1685–1690

Shoup TM, Eshima D, Eshima L, Olson J, Camp VM, Goodman MM (1997) Synthesis and evaluation of [F-18]-1-amino-3-fluorocyclopentane-1-carboxylic acid (FACPC) for tumor imaging and skeletal muscle metabolic studies by PET. J Nucl Med 38: 501

Shoup TM, Elmaleh DR, Bonab AA, Fischman AJ (2005) Evaluation of trans-9-^{18}F-fluoro-3,4-Methyleneheptadecanoic acid as a PET tracer for myocardial fatty acid imaging. J Nucl Med 46: 297–304

Simoes MV, Miyagawa M, Reder S, Stadele C, Haubner R, Linke W, Lehner T, Epple P, Anton M, Schwaiger M, Bengel FM (2005) Myocardial kinetics of reporter probe ^{124}I-FIAU in isolated perfused rat hearts after *in vivo* adenoviral transfer of herpes simplex virus type 1 thymidine kinase reporter gene. J Nucl Med 46: 98–105

Smith TA (1998) FDG uptake, tumour characteristics and response to therapy: a review. Nucl Med Commun 19: 97–105

Sokoloff L (1976) [1-^{14}C]-2-deoxy-d-glucose method for measuring local cerebral glucose utilization. Mathematical analysis and determination of the ''lumped'' constants. Neurosci Res Program Bull 14: 466–468

Sokoloff L, Reivich M, Kennedy C, Des Rosiers MH, Patlak CS, Pettigrew KD, Sakurada O, Shinohara M (1977) The [^{14}C]deoxyglucose method for the measurement of local cerebral glucose utilization: theory, procedure, and normal values in the conscious and anesthetized albino rat. J Neurochem 28: 897–916

Solin O, Eskola O, Hamill TG, Bergman J, Lehikoinen P, Gronroos T, Forsback S, Haaparanta M, Viljanen T, Ryan C, Gibson R, Kieczykowski G, Hietala J, Hargreaves R, Burns HD (2004) Synthesis and characterization of a potent, selective, radiolabeled substance-P antagonist for NK1 receptor quantitation: ([^{18}F]SPA-RQ). Mol Imaging Biol 6: 373–384

Spencer RP, Blau M (1962) Intestinal transport of selenium-75 selenomethionine. Science 136: 155–156

Stephan E, Pardo JV, Faris PL, Hartman BK, Kim SW, Ivanov EH, Daughters RS, Costello PA, Goodale RL (2003) Functional neuroimaging of gastric distention. J Gastrointest Surg 7: 740–749

Studenov AR, Szalda DE, Ding YS (2003) Synthesis of no-carrier-added C-11 labeled D- and L-enantiomers of phenylalanine and tyrosine for comparative PET Studies. Nucl Med Biol 30: 39–44

Sun KT, Chen K, Huang SC, Buxton DB, Hansen HW, Kim AS, Siegel S, Choi Y, Muller P, Phelps ME, Schelbert HR (1997) Compartment model for measuring myocardial oxygen consumption using [1-^{11}C]acetate. J Nucl Med 38: 459–466

Sun X, Fang H, Li X, Rossin R, Welch MJ, Taylor JS (2005) MicroPET imaging of MCF-7 tumors in mice via unr mRNA-targeted peptide nucleic acids. Bioconjug Chem 16: 294–305

Sundaresan G, Yazaki PJ, Shively JE, Finn RD, Larson SM, Raubitschek AA, Williams LE, Chatziioannou AF, Gambhir SS, Wu AM (2003a) ^{124}I-labeled engineered anti-CEA minibodies and diabodies allow high-contrast, antigen-specific small-animal PET imaging of xenografts in athymic mice. J Nucl Med 44: 1962–1969

Sundaresan G, Yazaki PJ, Shively JE, Finn RD, Larson SM, Raubitschek AA, Williams LE, Chatziioannou AF, Gambhir SS, Wu AM (2003b) I-124-labeled engineered Anti-CEA minibodies and diabodies allow high-contrast, antigen-specific small-animal PET imaging of xenografts in athymic mice. J Nucl Med 44: 1962–1969

Sundin A, Eriksson B, Bergstrom M, Langstrom B, Oberg K, Orlefors H (2004) PET in the diagnosis of neuroendocrine tumors. Ann NY Acad Sci 1014: 246–257

Surti S, Karp JS, Perkins AE, Freifelder R, Muehllehner G (2003) Design evaluation of A-PET: a high sensitivity animal PET camera. IEEE Trans Nucl Sci 50: 1357–1363

Susskind H, Alderson PO, Dzebolo NN, Bennett GW, Richards P, Rosen JM, Brill AB (1985) Effect of respiratory motion on pulmonary activity determinations by positron tomography in dogs. Invest Radiol 20: 950–955

Swanson JM, Volkow ND (2002) Pharmacokinetic and pharmacodynamic properties of stimulants: implications for the design of new treatments for ADHD. Behav Brain Res 130: 73–78

Tai YC, Chatziioannou AF, Yang YF, Silverman RW, Meadors K, Siegel S, Newport DF, Stickel JR, Cherry SR (2003) MicroPET II: design, development and initial performance of an improved microPET scanner for small-animal imaging. Phys Med Biol 48: 1519–1537

Tai YC, Ruangma A, Rowland D, Siegel S, Newport DF, Chow PL, Laforest R (2005) Performance evaluation of the microPET focus: a third-generation microPET scanner dedicated to animal imaging. J Nucl Med 46: 455–463

Takahashi T, Nishimura S, Ido T, Ishiwata K, Iwata R (1996) Biological evaluation of 5-methyl-branched-chain omega-[^{18}F]fluorofatty acid: a potential myocardial imaging tracer for positron emission tomography. Nucl Med Biol 23: 303–308

Takala TO, Nuutila P, Pulkki K, Oikonen V, Gronroos T, Savunen T, Vahasilta T, Luotolahti M, Kallajoki M, Bergman J, Forsback S, Knuuti J (2002) ^{14}(R,S)-[^{18}F]Fluoro-6-thia-heptadecanoic acid as a tracer of free fatty acid uptake and oxidation in myocardium and skeletal muscle. Eur J Nucl Med Mol Imaging 29: 1617–1622

Tang G, Wang M, Tang X, Luo L, Gan M (2003) Synthesis and evaluation of O-(3-[^{18}F]fluoropropyl)-L-tyrosine as an oncologic PET tracer. Nucl Med Biol 30: 733–739

Tavitian B (2003) *In vivo* imaging with oligonucleotides for diagnosis and drug development. Gut 52 [Suppl 4]: iv40–iv47

Tavitian B, Marzabal S, Boutet V, Kuhnast B, Terrazzino S, Moynier M, Dolle F, Deverre JR, Thierry AR (2002) Characterization of a synthetic anionic vector for oligonucleotide delivery using *in vivo* whole body dynamic imaging. Pharm Res 19: 367–376

Tawakol A, Migrino RQ, Hoffmann U, Abbara S, Houser S, Gewirtz H, Muller JE, Brady TJ, Fischman AJ (2005) Noninvasive *in vivo* measurement of vascular inflammation with F-18 fluorodeoxyglucose positron emission tomography. J Nucl Cardiol 12: 294–301

Thakur ML, Aruva MR, Gariepy J, Acton P, Rattan S, Prasad S, Wickstrom E, Alavi A (2004) PET imaging of oncogene overexpression using ^{64}Cu-vasoactive intestinal peptide (VIP) analog: comparison with 99mTc-VIP analog. J Nucl Med 45: 1381–1389

Toretsky J, Levenson A, Weinberg IN, Tait JF, Uren A, Mease RC (2004) Preparation of F-18 labeled annexin V: a potential PET radiopharmaceutical for imaging cell death. Nucl Med Biol 31: 747–752

Toyama H, Ichise M, Liow JS, Vines DC, Seneca NM, Modell KJ, Seidel J, Green MV, Innis RB (2004) Evaluation of anesthesia effects on [^{18}F]FDG uptake in mouse brain and heart using small animal PET. Nucl Med Biol 31: 251–256

Ugur O, Kothari PJ, Finn RD, Zanzonico P, Ruan S, Guenther I, Maecke HR, Larson SM (2002) Ga-66 labeled somatostatin analogue DOTA-DPhe1-Tyr3-octreotide as a potential agent for positron emission tomography imaging and receptor mediated internal radiotherapy of somatostatin receptor positive tumors. Nucl Med Biol 29: 147–157

Vaalburg W, Coenen HH, Crouzel C, Elsinga PH, Langstrom B, Lemaire C, Meyer GJ (1992) Amino acids for the measurement of protein synthesis *in vivo* by PET. Int J Radiat Appl Instrum B 19: 227–237

Vaalburg W, Hendrikse NH, de Vries EF (1999) Drug development, radiolabelled drugs and PET. Ann Med 31: 432–437

van den Hoff (2005) Principles of quantitative positron emission tomography. Amino Acids 29: 341–353

van Kouwen MC, Laverman P, van Krieken JH, Oyen WJ, Jansen JB, Drenth JP (2005) FDG-PET in the detection of early pancreatic cancer in a BOP hamster model. Nucl Med Biol 32: 445–450

van Nispen JW, Janssen WP, Melgers PA, Janssen PS, Jansen JF, Vaalburg W (1990) Synthesis and ^{11}C-labelling of the ACTH fragment analogue H-Met(O_2)-Glu-His-Phe-D-Lys-Phe-OH (Org 2766) via its homocystine-containing precursor. Int J Pept Protein Res 36: 167–172

Vaska P, Woody CL, Schlyer DJ, Shokouhi S, Stoll SP, Pratte JF, O'Connor P, Junnarkar SS, Rescia S, Yu B, Purschke M, Kandasamy A, Villanueva A, Kriplani A, Radeka V, Volkow N, Lecomte R, Fontaine R (2004) RatCAP: miniaturized head-mounted PET for conscious rodent brain imaging. IEEE Trans Nucl Sci 51: 2718–2722

Vavere AL, Laforest R, Welch MJ (2005) Production, processing and small animal PET imaging of titanium-45. Nucl Med Biol 32: 117–122

Verel I, Visser GW, Boerman OC, van Eerd JE, Finn R, Boellaard R, Vosjan MJ, Stigter-van Walsum M, Snow GB, van Dongen GA (2003) Long-lived positron emitters zirconium-89 and iodine-124 for scouting of therapeutic radioimmunoconjugates with PET. Cancer Biother Radiopharm 18: 655–661

Virgolini I, Traub-Weidinger T, Decristoforo C (2005) Nuclear medicine in the detection and management of pancreatic islet-cell tumours. Best Pract Res Clin Endocrinol Metab 19: 213–227

Visser FC (2001) Imaging of cardiac metabolism using radiolabelled glucose, fatty acids and acetate. Coron Artery Dis 12 [Suppl 1]: S12–S18

Wang HE, Wu SY, Chang CW, Liu RS, Hwang LC, Lee TW, Chen JC, Hwang JJ (2005) Evaluation of F-18-labeled amino acid derivatives and [^{18}F]FDG as PET probes in a brain tumor-bearing animal model. Nucl Med Biol 32: 367–375

Washburn LC, Sun TT, Wieland BW, Hayes RL (1977) C-11-Dl-tryptophan, a potential pancreas imaging agent for positron tomography. J Nucl Med 18: 638

Washburn LC, Sun TT, Byrd BL, Callahan AP (1982) Production of L-[1-^{11}C]valine by HPLC resolution. J Nucl Med 23: 29–33

Weber S, Terstegge A, Herzog H, Reinartz R, Reinhart P, Rongen F, Muller-Gartner HW, Halling H (1997) The design of an animal PET: flexible geometry for achieving optimal spatial resolution or high sensitivity. IEEE Trans Med Imaging 16: 684–689

Weber WA, Wester HJ, Grosu AL, Herz M, Dzewas B, Feldmann HJ, Molls M, Stocklin G, Schwaiger M (2000) O-(2-[^{18}F]fluoroethyl)-L-tyrosine and L-[methyl-^{11}C]methionine uptake in brain tumours: initial results of a comparative study. Eur J Nucl Med 27: 542–549

Weber S, Bauer A (2004) Small animal PET: aspects of performance assessment. Eur J Nucl Med Mol Imaging 31: 1545–1555

Wester HJ, Dittmar C, Herz M, SenekowitschSchmidtke R, Schwaiger M, Stocklin G (1997) Synthesis and biological evaluation of O-(2-[F-18]fluoro-ethyl)-(L)-tyrosine (FET): a potential PET tracer for amino acid transport. J Nucl Med 38: 756

Wester HJ, Herz M, Weber W, Heiss P, Senekowitsch-Schmidtke R, Schwaiger M, Stocklin G (1999) Synthesis and radiopharmacology of O-(2-[^{18}F]fluoroethyl)-L-tyrosine for tumor imaging. J Nucl Med 40: 205–212

Wester HJ, Schottelius M, Scheidhauer K, Meisetschlager G, Herz M, Rau FC, Reubi JC, Schwaiger M (2003) PET imaging of somatostatin receptors: design, synthesis and preclinical evaluation of a novel ^{18}F-labelled, carbohydrated analogue of octreotide. Eur J Nucl Med Mol Imaging 30: 117–122

Whitford GM, Pashley DH (1984) Fluoride absorption: the influence of gastric acidity. Calcif Tissue Int 36: 302–307

Wild D, Macke HR, Waser B, Reubi JC, Ginj M, Rasch H, Muller-Brand J, Hofmann M (2005) ^{68}Ga-DOTANOC: a first compound for PET imaging with high affinity for somatostatin receptor subtypes 2 and 5. Eur J Nucl Med Mol Imaging 32: 724

Wolf AP, Redvanly CS (1977) Carbon-11 and radiopharmaceuticals. Int J Appl Radiat Isot 28: 29–48

Wright PL (1965) Life span of ovine erythrocytes as estimated from selenium-75 kinetics. J Anim Sci 24: 546–550

Wu HM, Huang SC, Allada V, Wolfenden PJ, Schelbert HR, Phelps ME, Hoh CK (1996) Derivation of input function from FDG-PET studies in small hearts. J Nucl Med 37: 1717–1722

Wu AM, Yazaki PJ, Tsai S, Nguyen K, Anderson AL, McCarthy DW, Welch MJ, Shively JE, Williams LE, Raubitschek AA, Wong JY, Toyokuni T, Phelps ME, Gambhir SS (2000a) High-resolution micro-PET imaging of carcinoembryonic antigen-positive xenografts by using a copper-64-labeled engineered antibody fragment. Proc Natl Acad Sci USA 97: 8495–8500

Wu F, Orlefors H, Bergstrom M, Antoni G, Omura H, Eriksson B, Watanabe Y, Langstrom B (2000b) Uptake of ^{14}C- and ^{11}C-labeled glutamate, glutamine and aspartate *in vitro* and *in vivo*. Anticancer Res 20: 251–256

Wu F, Yngve U, Hedberg E, Honda M, Lu L, Eriksson B, Watanabe Y, Bergstrom M, Langstrom B (2000c) Distribution of ^{76}Br-labeled antisense oligonucleotides of different length determined ex vivo in rats. Eur J Pharm Sci 10: 179–186

Wuest F (2005) Aspects of positron emission tomography radiochemistry as relevant for food chemistry. Amino Acids 29: 323–339

Yagle KJ, Eary JF, Tait JF, Grierson JR, Link JM, Lewellen B, Gibson DF, Krohn KA (2005) Evaluation of ^{18}F-annexin V as a PET imaging agent in an animal model of apoptosis. J Nucl Med 46: 658–666

Yamamoto F, Nakada K, Zhao S, Satoh M, Asaka M, Tamaki N (2004) Gastrointestinal uptake of FDG after N-butylscopolamine or omeprazole treatment in the rat. Ann Nucl Med 18: 637–640

Yang Y, Tai YC, Siegel S, Newport DF, Bai B, Li Q, Leahy RM, Cherry SR (2004) Optimization and performance evaluation of the microPET II scanner for *in vivo* small-animal imaging. Phys Med Biol 49: 2527–2545

Yang D, Han L, Kundra V (2005) Exogenous gene expression in tumors: noninvasive quantification with functional and anatomic imaging in a mouse model. Radiology 235: 950–958

Yao R, Seidel J, Johnson CA, Daube-Witherspoon ME, Green MV, Carson RE (2000) Performance characteristics of the 3-D OSEM algorithm in the reconstruction of small animal PET images. Ordered-subsets expectation-maximixation. IEEE Trans Med Imaging 19: 798–804

Yoshimoto M, Waki A, Yonekura Y, Sadato N, Murata T, Omata N, Takahashi N, Welch MJ, Fujibayashi Y (2001) Characterization of acetate metabolism in tumor cells in relation to cell proliferation: acetate metabolism in tumor cells. Nucl Med Biol 28: 117–122

Younes CK, Boisgard R, Tavitian B (2002) Labelled oligonucleotides as radiopharmaceuticals: pitfalls, problems and perspectives. Curr Pharm Des 8: 1451–1466

Yudilevich DL (1989) Blood-tissue transport of substrates in the heart: studies by single circulation tracer dilution. Int J Microcirc Clin Exp 8: 397–409

Zhang H, Chen J, Waldherr C, Hinni K, Waser B, Reubi JC, Maecke HR (2004) Synthesis and evaluation of bombesin derivatives on the basis of pan-bombesin peptides labeled with indium-111, lutetium-177, and yttrium-90 for targeting bombesin receptor-expressing tumors. Cancer Res 64: 6707–6715

Ziemons K, Auffray E, Barbier R, Brandenburg G, Bruyndonckx P, Choi Y, Christ D, Costes N, Declais Y, Devroede O, Dujardin C, Fedorovd A, Heinrichs U, Korjik M, Krieguer M, Kuntner C, Largeron G, Lartizien C, Larue H, Lecoq P, Leonard S, Marteau J, Morel C, Mosset JB, Parl C, Pedrini C, Petrosyan AG, Pietrzyk U, Rey M, Saladino S, Sappey-Marinier D, Simon L, Streun M, Tavernier S, Vieira JM (2005) The ClearPET (TM) project: development of a 2nd generation high-performance small animal PET scanner. Nuclear Instruments & Methods in Physics Research Section A – Accelerators, Spectrometers, Detectors and Associated Equipment 537: 307–311

Zijlstra S, Gunawan J, Burchert W (2003) Synthesis and evaluation of a ^{18}F-labelled recombinant annexin-V derivative, for identification and quantification of apoptotic cells with PET. Appl Radiat Isot 58: 201–207

Zubieta JK, Dannals RF, Frost JJ (1999) Gender and age influences on human brain mu-opioid receptor binding measured by PET. Am J Psychiatry 156: 842–848

Authors' address: Ralf Bergmann, PhD, PET Center, Institute of Bioinorganic and Radiopharmaceutical Chemistry, Research Center Rossendorf, P. O. Box 51 01 19, 01314 Dresden, Germany,
Fax: 0049 351 260 1 3097, E-mail: r.bergmann@fz-rossendorf.de